Journal of Neurochemistry

WILEY | ISN International Society for Neurochemistry

ORIGINAL ARTICLE OPEN ACCESS

SPECIAL ISSUE Microbiota and Gut-Brain Axis

Lack of Structural Change in Olfactory Circuitry Following Fecal Microbiome Transplant From Donors Subjected to Diet-induced Obesity

Ashley M. Loeven[1] | Franklin A. Pacheco[1] | Amber N. Brown[2] | Debra Ann Fadool[1,3,4]

[1]Department of Biological Science, The Florida State University, Tallahassee, Florida, USA | [2]Department of Biological Science Core Facilities, The Florida State University, Tallahassee, Florida, USA | [3]Program in Neuroscience, The Florida State University, Tallahassee, Florida, USA | [4]Institute of Molecular Biophysics, The Florida State University, Tallahassee, Florida, USA

Correspondence: Debra Ann Fadool (dfadool@bio.fsu.edu)

Received: 15 August 2025 | **Revised:** 10 January 2026 | **Accepted:** 7 February 2026

Keywords: dysbiosis | gut | metabolism | microbiome | obesity | olfaction

ABSTRACT

Obesity and fatty diets are known to damage the structure and function of chemosensory systems. Consumption of a moderately high-fat diet (MHF) induces loss of olfactory sensory neurons (OSNs) and reduces the density of associated axonal projections to the olfactory bulb that are central in the coding of odor information. Previous work has demonstrated reduced alpha diversity, as well as signature changes in microbiome composition when mice are challenged with a MHF diet that precipitates diet-induced obesity. Herein, we tested the hypothesis that a dysbiotic gut microbiome is sufficient to induce olfactory damage. Male and female donor mice were randomly assigned to a control-fat (CF) or MHF diet for 5 months duration, followed by baseline measurements of body weight, body composition (EchoMRI), glucose tolerance, and metabolic phenotyping via indirect calorimetry. We next performed fecal microbiome transplantation (FMT) from these donors to CF-maintained recipient mice. After 8 weeks post FMT, we observed no difference in body weight, glucose clearance, body composition, or fat pad weights as a consequence of transfer from MHF-maintained donors. Following FMT, recipient male mice exhibited increased *Erysipelotrichaceae* abundance and decreased *Lactobacillaceae* abundance, similar to MHF-fed donors. Recipient brains were processed for tissue clearing using immunolabeling-enabled three-dimensional imaging of solvent-cleared organs (iDISCO) and then imaged using high resolution light sheet microscopy. The volume of olfactory glomeruli expressing Olfr160 odor receptors could be visualized using genetic reporters; the FMT from MHF-maintained donors failed to evoke structural changes to these defined olfactory synapses. We conclude that diet-induced obesity, associated adiposity, and metabolic dysfunctions drive functional loss and structural changes to the olfactory system, but that gut microbiome dysbiosis alone is not sufficient to yield olfactory circuitry deficits.

Abbreviations: 2-w RM ANOVA, 2-way repeated measures ANOVA; Abx, antibiotic; AVMA, American Veterinary Medical Association; BAT, brown adipose tissue; CF, control-fat chow; CLAMS, Comprehensive Laboratory Animal Monitoring System; DIO, diet-induced obesity; DMSO, dimethyl sulfoxide; EE, energy expenditure; FMT, fecal microbiome transplantation; FMT-CF, fecal microbiome transplantation using CF-fed donor fecal material; FMT-MHF, fecal microbiome transplantation using MHF-fed donor fecal material; FSU, Florida State University; GAC, goat anti-chicken; h, hour; IACUC, Institutional Animal Care and Use Committee; iAUC, integrated area under the curve; iDISCO, immunolabeling-enabled three-dimensional imaging of solvent-cleared organs; IPGTT, intraperitoneal glucose tolerance test; MHF, moderately high-fat chow; NIH, National Institutes of Health; OB, olfactory bulb; Olfr160, olfactory receptor 160; OSN, olfactory sensory neuron; P, postnatal day; PBS, phosphate buffered saline; QIIME2, Quantitative Insights into Microbial Ecology; RER, respiratory exchange ratio; ROI, region of interest; RRID, Research Resource Identifier (see scicrunch.org); SD, standard deviation; VCO_2, carbon dioxide production; VO_2, oxygen consumption; WAT, white adipose tissue.

This is an open access article under the terms of the Creative Commons Attribution-NonCommercial-NoDerivs License, which permits use and distribution in any medium, provided the original work is properly cited, the use is non-commercial and no modifications or adaptations are made.

© 2026 The Author(s). *Journal of Neurochemistry* published by John Wiley & Sons Ltd on behalf of International Society for Neurochemistry.

1 | Introduction

Obesity is a chronic disease characterized by low-grade systemic inflammation as well as excess adiposity that puts individuals at higher risk for conditions such as type 2 *diabetes mellitus* and metabolic syndrome (Chandrasekaran and Weiskirchen 2024; Engin and Engin 2017). Obesity is driven by energy imbalance, and chemosensory changes observed in obesity may further drive dysregulated feeding behaviors (Ferrario et al. 2024; Harnischfeger and Dando 2021). While it is well known that obesity, unhealthy diet, and metabolic imbalance have deleterious effects on the structure and function of our chemosensory systems (Fathi et al. 2023; Islam et al. 2015; Liu, Archer, et al. 2016; Matiashova et al. 2023; Peinado et al. 2023; Peng et al. 2019; Proserpio et al. 2015; Şeref and Yıldıran 2024; Trius-Soler et al. 2020), the cellular mechanism of loss is less understood. Diet-induced obesity is associated with loss of taste buds (Kaufman et al. 2018), loss of fungiform papillae (Kaufman et al. 2020), reduced numbers of olfactory sensory neurons (Chelette et al. 2022; Thiebaud et al. 2014), and fewer axonal projections to the olfactory bulb (Chelette et al. 2022; Thiebaud et al. 2014). In both olfaction and gustation, consumption of high-fat diet is associated with increased inflammation, reduced cell birth, and increased cell death (Chelette et al. 2022; Kaufman et al. 2018; Thiebaud et al. 2014).

Interestingly, in the olfactory system, loss of olfactory sensory neurons attributed to diet-induced obesity does not recover following return to a low-fat diet (Thiebaud et al. 2014). The high-fat diet causes an upregulation of genes associated with mRNA metabolic processes, DNA damage responses, and DNA repair within the olfactory bulb (Kim et al. 2025). Moreover, mice subjected to diet-induced obesity exhibit a reduction in electroolfactogram amplitude, irregular excitability of action potential firing of output neurons in the olfactory bulb, and reduced discrimination between odor molecules (Fadool et al. 2011; Thiebaud et al. 2014; Tucker et al. 2010). In an isocaloric pair-feeding paradigm where fat-fed mice remain lean, loss of olfactory sensory neurons persists, suggesting that neuronal loss can be driven by the diet itself independent of obesity (Chelette et al. 2022).

Diet is a major modulator of gut microbiome composition, and the gut microbiome plays a role in whole-body physiology. Obesity markedly disrupts the gut microbiome, inducing gut microbiome dysbiosis (de La Serre et al. 2010; Ley et al. 2005; Nagpal et al. 2020; Ridaura et al. 2013; Turnbaugh et al. 2006, 2008). Fecal microbiome transplantation (FMT) experiments suggest that the gut microbiome regulates body fat deposition (Bäckhed et al. 2004; Turnbaugh et al. 2006), as well as behaviour, neuroinflammation, and neuronal loss (Bruce-Keller et al. 2015; D'Amato et al. 2020; Kelly et al. 2016; Kim et al. 2020, 2023; Li et al. 2019). Because the gut microbiome is sufficient to transmit negative health outcomes associated with obesity and fatty diets, we wondered if transfer of a gut microbiome obtained from an obese donor could transmit damage to the olfactory system, in an otherwise healthy recipient.

To this end, we tested how fecal microbiome transplantation from fat-fed mice could elicit changes in metabolism, body composition, and olfactory circuitry. Donor material was collected from male and female mice maintained on a moderately high-fat diet for 5 months. Male mice exhibited diet-induced obesity, glucose intolerance, increased adiposity, and metabolic dysfunction. Female mice were resistant to diet-induced obesity, exhibited glucose sensitivity, but had changes in body composition. Transplantation of fecal matter to control-fed, recipient mice caused anticipated changes in microbiota in the male mice, without any sustained changes in body weight, glucose tolerance, or adiposity over the course of the 8-week exposure in either the male or female mice. Light sheet microscopy was utilized to investigate the volume of Olfr160 glomeruli, as loss of Olfr160 olfactory sensory neurons and associated projections has been previously reported following diet-induced obesity (Chelette et al. 2022; Thiebaud et al. 2014). Despite the observed gut dysbiosis in male mice, recipient mice of both sexes had no reduction in the size of the Olfr160 olfactory glomerulus. Overall, these data suggest that the dysbiotic gut microbiome is not sufficient to induce metabolic and olfactory anatomical changes in the absence of excess dietary fat or obesity.

2 | Materials and Methods

Our study design was not pre-registered as a clinical trial.

2.1 | Ethics Statement

All animal experiments were approved by the Florida State University (FSU) Institutional Animal Care and Use Committee (IACUC) under protocol #202000036 and were conducted in accordance with the American Veterinary Medicine Association (AVMA) and the National Institutes of Health (NIH). In preparation for optically clearing the brain, mice were anesthetized with a mixture of ketamine hydrochloride (80 mg/kg, Covetrus, Portland, ME, USA) and xylazine hydrochloride (10 mg/kg, MWI Veterinary Supply, Boise, ID, USA) and were sacrificed by cardiac exsanguination followed by decapitation (Leary et al. 2020).

2.2 | Animal Care and Diet

Mice were maintained on a reverse 12-h light/dark cycle to facilitate experimentation during the dark cycle. Animals were individually housed in open, conventional-style rodent cages in the FSU *vivarium* with two forms of environmental enrichment. Individual housing, although beneficial for social dynamics, was necessary for metabolic monitoring, glucose tolerance testing, olfactory circuitry development, and increased gut microbiome variability among donor animals due to the coprophagic nature of mice. Mice were provided *ad libitum* access to food and water unless otherwise noted, and cages were changed once weekly.

Mice were maintained on either control-fat chow (CF) containing 13.6% kcal fat, 57.5% kcal carbohydrate, and 28.9% kcal protein (Rodent Diet 5001, LabDiet, St. Louis, Missouri, USA), or moderately high-fat chow (MHF) containing 31.8% kcal fat, 51.4% kcal carbohydrate, and 16.8% kcal protein (Catalog #D12266B, Research Diets, New Brunswick, New Jersey, USA). Donor animals were arbitrarily assigned to, and then maintained on, one of these two diets starting at postnatal day 28 (male (14.1 ± 2.6 g;

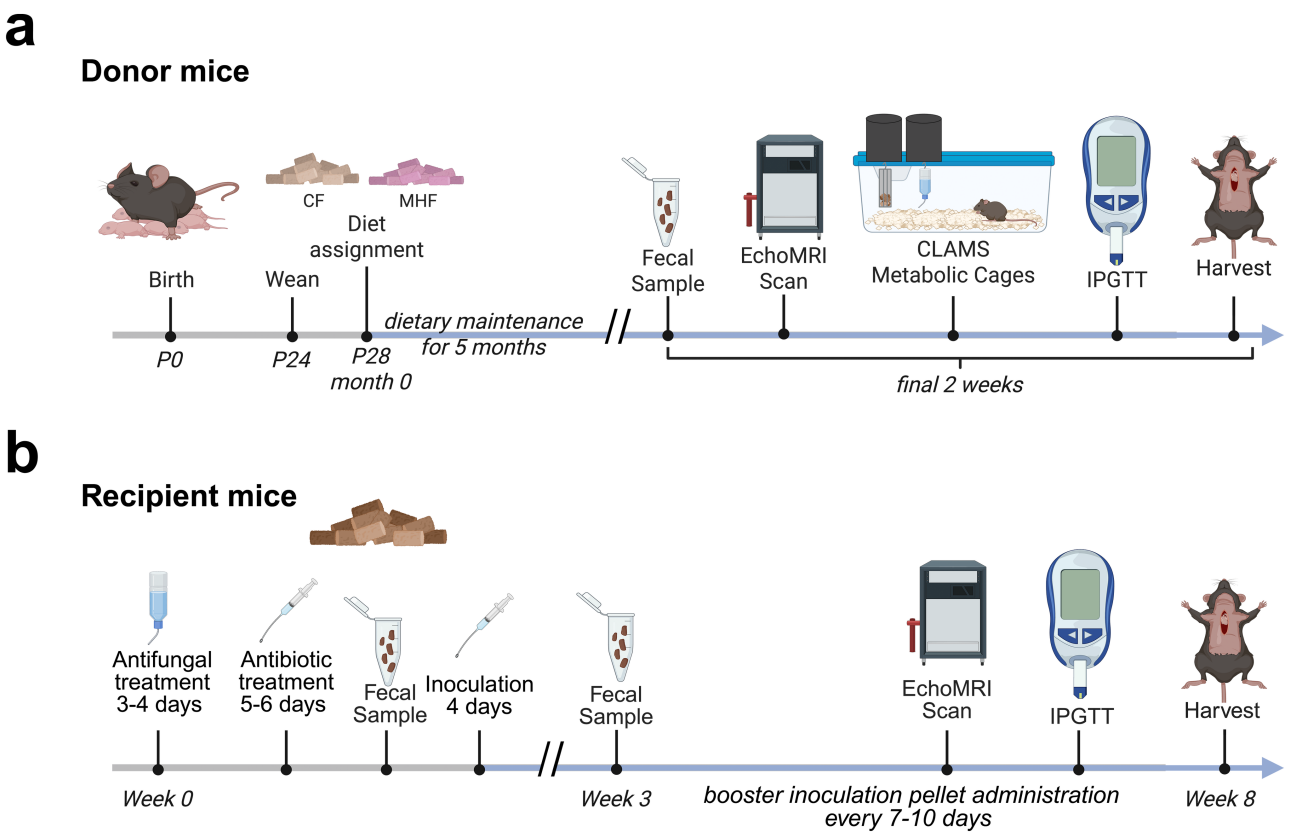

FIGURE 1 | Experimental timeline of fecal microbiome transplantation. (a) Donor mice were bred in-house and weaned at postnatal Day 24 (P24). Mice were assigned to either control-fat (CF, 13% kcal/fat) or moderately high-fat (MHF, 31.8% kcal/fat) chow *ad libitum* at P28. Mice were maintained on their assigned diet for 5 months. During the final 2 weeks of treatment, mice underwent fecal sampling, EchoMRI scanning, metabolic phenotyping (CLAMS), intraperitoneal glucose tolerance testing (IPGTT), and then were sacrificed for post-mortem tissue analyses (Harvest). (b) Recipient mice underwent antifungal treatment (3–4 days), antibiotic treatment (5–6 days), and inoculation with donor material (4 days). Fecal samples were collected to confirm depletion of fecal bacteria and reinoculation of gut bacteria (3 weeks after transplant). Booster inoculation occurred through week 8 (see Figure 6). Mice underwent EchoMRI scanning, IPGTT and then were sacrificed for post-mortem tissue analyses (Harvest) during the final 2 weeks (in a similar fashion as (a.); 7–8 weeks after transplant). Created in BioRender. Loeven, A. (2026) https://BioRender.com/s314vyj.

$n = 30$) and female (13.1 ± 1.9 g; $n = 29$); mean ± SD), which continued for 5 months (Figure 1a). Body weights were collected weekly during dietary maintenance. Recipient mice were weaned and then maintained on CF (Figure 1b) prior to antibiotic depletion at 5–6 months of age. The full sequence of experiments performed on donor and recipient mice can be found in Figure 1.

2.3 | Experimental Animals

All donor mice were a C57BL6/J background—pooled from two different strains used previously in the laboratory and known to have identical response to maintenance on MHF diets, namely wildtype mice (RRID: IMSR_JAX:000664; The Jackson Laboratory, Bar Harbor, Maine, USA, strain #000664) and mice with an olfactory reporter for the Olfactory Receptor 160 (Olf160; M72-IRES-*tau*LacZ, RRID: IMSR_JAX:006596; The Jackson Laboratory, strain #006596 (Zheng et al. 2000)). Recipient mice (Olfr160; M72-IRES-*tau*GFP, RRID: IMSR_JAX:006678, The Jackson Laboratory, strain #006678 (Potter et al. 2001)) contained the same olfactory reporter for Olfactory Receptor 160, with the exception that the internal ribosome entry site used a *tau*GFP rather than a *tau*LacZ to enable optical visualization of the receptor in expressing olfactory sensory neurons (generously provided by Dr. Thomas Bozza, Northwestern University, Chicago, Illinois, USA) that was suitable for immunolabeling-enabled three-dimensional imaging of solvent-cleared organs (iDISCO).

A total of 83 mice (40 male, 43 female) were used in this study and were arbitrarily assigned to either CF diet or MHF diet. Of the 83 mice, 24 mice underwent fecal microbiome transplantation, and 19 of the 59 mice (as above) served as donors. One male MHF-fed mouse died during Week 20 of diet maintenance of unknown causes and was not replaced as a donor mouse. One male recipient mouse was euthanized following oral gavage and was not replaced for transplantation.

2.4 | Solutions and Antisera

All salts, detergents and chemicals were obtained from Fisher Scientific/Thermo Scientific (Waltham, MA, USA) or Sigma Chemical (Atlanta, GA, USA) unless otherwise noted. Phosphate buffered saline (PBS), used in tissue preparation,

was made as described previously (Tucker and Fadool 2002) and contained: 137 mM NaCl, 2.7 mM KCl, 10 mM Na_2HPO_4 (Macron Chemicals, now part of Avantor, Radnor Township, PA, USA), and 1.8 mM KH_2PO_4. Brain tissue was cleared using the iDISCO protocol, which required several tissue processing solutions (Kimbrough and George 2020; Renier et al. 2014). Ptx.2 solution was comprised of 0.2% Triton X-100 in 1× PBS. PtWH solution was comprised of 0.2% Tween-20 plus 0.1 mg/L heparin (Sigma Aldrich, St Louis, MO) in 1× PBS. Permeabilization solution contained 306.4 mM glycine in 20% dimethyl sulfoxide (DMSO) and 80% Ptx.2. Blocking solution contained 84% Ptx.2, 10% DMSO, and 6% normal goat serum. GFP+ neurons were labeled with a polyclonal chicken anti-GFP (1:1000 GFP-1020; RRID: AB_10000240; AvesLabs Davis, CA, USA; https://idisco.info/validated-antibodies/(Bray et al. 2017; Lozovaya et al. 2018; Moore et al. 2019)) mixed with 5% DMSO and 3% normal goat serum in PtWH. Secondary antibody labelling was achieved by incubation of AlexaFluor 488 goat anti-chicken (GAC) secondary antibody (1:200, IgY (H + L), Catalog# A-11039, RRID: AB_2534096; ThermoFisher Scientific) in 3% normal goat serum in PtWH.

2.5 | Body Composition

Mice were scanned in an EchoMRI-900 (EchoMRI LLC, Houston, TX, USA) to measure lean and fat mass without the requirement for anesthesia 4–7 h into the dark cycle. Mice were guided into a long restraint cylinder while a second, narrower cylinder was inserted and secured in place to prevent excessive movement. The cylinder was placed into the EchoMRI, and the scan (30 s to 3 min) was performed to determine the live mass measurement.

2.6 | Glucose Tolerance

Mice underwent an intraperitoneal glucose tolerance test (IPGTT) to determine diabetic state (University of Virginia Vivarium Protocols, Susanna R. Keller). Mice underwent a 12-h light cycle fast. Glucose was intraperitoneally delivered (at time 0, onset of dark cycle) using a 25% (w/v) D-(+)-glucose (Sigma Aldrich) solution at a dose of 1 g of glucose per kg of body weight. The tip of the tail was cut for blood collection, and a single droplet was used to fill the glucose meter at each time point. The total amount of blood collected from each subject is estimated to be less than 10 μL. Blood was collected at time −10 (fasted baseline), 10, 20, 30, 60, 90, and 120 min. Blood glucose was measured using a Contour Next Blood Glucose Monitoring System (Ascensia Diabetes Care US Inc., Parsippany, NJ, USA). Blood glucose values (mg/dL) were plotted against time, and the area under the curve was integrated (iAUC).

2.7 | Metabolic Phenotyping

Mice were placed into a Comprehensive Laboratory Animal Monitoring System (CLAMS, Columbus Instruments, Columbus, OH, USA) for metabolic assessment. The CLAMS system uses indirect calorimetry to measure oxygen consumption (VO_2; mL/kg/h), carbon dioxide production (VCO_2; ml/kg/h), respiratory exchange ratio (RER), and energy expenditure (EE; kcal/h) and also can compute locomotor activity. VO_2 and VCO_2 were normalized with respect to body weight in kilograms. RER was calculated as VCO_2/VO_2. EE was calculated using the Lusk Graham equation (3.815 + 1.232 × RER) × VO_2 (Lusk and Du Bois 1924). Locomotor activity was measured with optical beams along the *x*-axis of the cage. Beam breaks were interpreted as ambulatory movement. Mice were fed via hanging feeders and water bottles attached to scales. Metabolic and ambulatory data were recorded with Oxymax software on a rotation with 18 min between measurements of a single cage and a 30-s sampling period for each cage. Mice were housed in the CLAMS for a total of 5–6 days (2–3 days of acclimation and 3 full days of data collection).

2.8 | Fecal Sampling and Processing for Transplantation

Fecal samples were collected from mice (±4 h (h) from dark cycle onset) for gut microbiome analysis and transplantation. For fecal collections mice were individually placed into disinfected cage bottoms (up to ~3 h) without bedding, and without access to food and water for the sampling duration. Fecal pellets were collected using individual, autoclaved wooden sticks, and placed into microcentrifuge tubes. Processing time was variable but was spread across groups evenly (i.e., collections from CF- and MHF-treated mice were utilized at the same time).

Fecal pellet collections destined for DNA extraction and sequencing (see next section) were stored dry at −80°C until day of use. Fecal pellet collections destined for gut microbiome transplantation via oral gavage were first held on ice and then diluted 100 mg/mL in 20% glycerol (v/v) (Fisher Scientific) in 1× PBS. Pellets were crudely homogenized with autoclaved wooden sticks, vortexed, and maintained on ice. Resuspended fecal matter was centrifuged at 500× *g* for 5 min at 4°C to remove particulate matter. The resulting supernatant was aliquoted on ice and stored at −80°C until utilized for FMT.

Additional fecal pellets for gut microbiome transplantation via non-invasive pellet administration were collected by placing mice into fresh caging for 1–5 days. After the collection period, mice were removed into fresh caging and fecal pellets were collected and stored at −80°C. Pellets were used for non-invasive "booster" reinoculation of the donor gut microbiome provided to recipient mice every 7–10 days following initial inoculation via oral gavage (see Figure 1b).

2.9 | DNA Extraction and 16 s v4 Sequencing

DNA was extracted from stored fecal pellets (1–2 pellets/sample) using Qiagen QIAamp PowerFecal Pro DNA Kit (Catalog #51804; Hilden, Germany) as per the manufacturer's instructions. Extracted DNA was processed for sequencing by the FSU Department of Biological Science Molecular Core Facility. Briefly, the V4 hypervariable region of the 16 s rRNA gene was amplified by PCR using region-specific, barcoded primers and targeted for paired-end (2 × 251 base pair) sequencing by

Illumina MiSeq (San Diego, California, USA) according to the Earth Microbiome Project (Caporaso et al. 2011, 2012).

2.10 | Fecal Microbiota Transplant (FMT)

Mice that were 5.7 months old (±1.8 months; body weight (grams) male: 31.9 ± 2.9; female: 25.4 ± 2.7) underwent fecal microbiome transplantation (FMT) as previously described (Kadyan et al. 2023; Kim et al. 2020) with slight modification. Antibiotics and fecal matter homogenates were administered by oral gavage (22-gauge feeding needle Catalog #18061–22, curved to enter the esophagus smoothly; Fine Science Tools, Foster City, CA, USA). A total of 19 donor animals (10 female: 5 CF, 5 MHF; 9 male: 5 CF, 4 MHF) provided fecal material for transplantation. A final total of 23 CF animals served as recipients, whereby the mice received the following type of diet-maintained donor fecal matter (14 female: 7 CF, 7 MHF; 9 male: 4 CF, 5 MHF). Recipients received fecal material from a single donor mouse (donor material was not pooled). 4 female donors (2 CF, 2 MHF) provided material for 2 recipient animals instead of 1. Gavage was not performed more than once daily. To prevent fungal overgrowth, mice were first provided *ad libitum* antifungal water (Amphotericin-B, 0.01 g/L, Catalog #A-560, GoldBio, St. Louis, MO, USA) for 3–4 days prior to antibiotic administration. All antibiotics were acquired from GoldBio and were administered as a mixture for 5–6 days to include: Ampicillin Sodium (100 mg/kg, Catalog #A-301), Gentamicin Sulfate (100 mg/kg, Catalog #G-400), Metronidazole (100 mg/kg, Catalog #M-295), Neomycin Sulfate (100 mg/kg, Catalog #N-620), and Vancomycin Hydrochloride (50 mg/kg, Catalog #V-200). Following bacterial depletion, mice then received daily administration of donor material (30 μL prepared fecal homogenate mixed with 130 μL 1× PBS) for 4 days. Mice were observed for at least 15 min following each oral gavage for signs of pain, distress, or unusual respiratory rate/pattern. Body weight was monitored daily throughout antifungal, antibiotic, and donor material administration.

2.11 | Post-Mortem Tissue Harvesting and Clearing

Mice were anesthetized with a mixture of ketamine hydrochloride (80 mg/kg, Covetrus, Portland, ME, USA) and xylazine hydrochloride (10 mg/kg, MWI Veterinary Supply, Boise, ID, USA). Anesthetic depth was confirmed by reduced respiratory rate and lack of response to toe pinch. Mice were exsanguinated by cardiac perfusion first with 1× PBS solution, then 4% (w/v) paraformaldehyde (Catalog #A11313.36, Fisher Scientific) in 1× PBS solution. Skulls were post-fixed for 3 h at 4°C, washed 3 times in 1× PBS, then decalcified in 0.3 M ethylenediaminetetraacetic acid disodium salt dihydrate at 4°C. Post-mortem adipose tissue deposits (subcutaneous white adipose tissue, mesenteric white adipose tissue, retroperitoneal white adipose tissue, gonadal white adipose tissue, intrascapular brown adipose tissue), liver and spleen were dissected and weighed as performed previously (Chelette et al. 2022; Tucker et al. 2012).

A 16-day iDISCO+ protocol was used to optically clear the harvested olfactory bulbs (OBs) (Kimbrough and George 2020; Renier et al. 2014). All washes were performed for 1 h at room temperature unless otherwise noted. The OB tissue was first dehydrated in a series of methanol/water (v/v) dilutions (20%, 40%, 60%, 80%, 100%, 100%). The OBs were incubated in 66% dichloromethane (Sigma-Aldrich) and 33% methanol overnight. The following day, the OBs were washed in 100% methanol twice, chilled, and incubated in 5% hydrogen peroxide in methanol overnight at 4°C. OBs were rehydrated the following day (80%, 60%, 40%, 20%, PBS, Ptx.2, Ptx.2) before incubating in permeabilization solution at 37°C for 2 days. Samples were incubated in blocking solution for 2 days at 37°C. Next, the OBs were incubated in the GFP-1020 primary antibody solution for 3 days at 37°C. The OBs were then washed in PtWH for 5 washes and left in the final wash overnight. The following day, the OBs were incubated in the anti-GAC secondary antibody solution for 3 days at 37°C. Tissue was again rinsed in PtWH for 5 washes and left in the final wash overnight. Samples were dehydrated with 20%, 40%, 60%, 80%, 100%, 100% methanol dilutions and left in the final wash overnight. Finally, the OBs were cleared by incubating in 66% dichloromethane/33% methanol for 3 h, followed by two 15-min 100% dichloromethane washes. OBs were stored in dibenzyl ether (Sigma-Aldrich) in the dark at room temperature until imaged.

2.12 | Microscopy and Image Analysis

Prior to tissue clearing, whole-mount images of the olfactory bulbs were acquired on a Nikon AZ100M stereoscope (Nikon, Melville, New York, USA) outfitted with a Nikon AZ Plan Fluor 5× objective and a Nikon DS Qi1Mc Camera using the Nikon NIS-Elements platform. The lateral glomerular area was estimated using the open-source software Fiji (Schindelin et al. 2012). The area was estimated using the region of interest (ROI) freehand selection tool and quantifying the pixels within that ROI. The medial glomeruli could not reliably be observed using this method and thus were not imaged. iDISCO-cleared olfactory bulbs were imaged using a LaVision BioTec Ultramicroscope II light sheet microscope (Miltenyi Biotec, Waltham, MA, USA) in dibenzyl ether. Z-stacks were collected using a 2-μm step size at 3.2× magnification with a 488 nm laser wavelength on a metal-oxide semiconductor PCO Edge Camera (PCO; Kelheim, Germany). Glomerular volume for both the lateral and medial Olfr160 glomeruli was estimated using Fiji (Schindelin et al. 2012) with the Measure Stack plugin called OptiNav (Dougherty 2002). Glomerular images were labeled with animal ID (genotype, number, and sex; no experimental treatment) and investigators were blind to experimental treatment during imaging and analysis. The olfactory bulbs of one FMT MHF female mouse remained cloudy after clearing, so images were not quantified. Images were reduced to 400 × 800 pixels and edited for brightness and contrast in Fiji.

2.13 | Microbiome Analysis

Bacterial sequences were processed in the Quantitative Insights into Microbial Ecology (QIIME2, version 2022.11, 2025.10) (Bolyen et al. 2019) pipeline, demultiplexed, and denoised (soft cutoff of median quality score of 20) using DADA2 (Callahan et al. 2016), and then assigned to taxa using the Greengenes2 database (2024.09, 2024.09.backbone.full-length.nb.sklearn-1.4.2 classifier (Bokulich et al. 2018; McDonald et al. 2024)). Data

were rarefied to 12,000 reads/sample to retain all samples at minimum sampling depth (minimum 12,806, maximum 61,407, Figure S1). Taxonomic data were exported and imported into MicrobiomeAnalyst 2.0 (rarefied to 12,806 reads/sample, without additional filtering, normalization, scaling, or transforming) (Lu et al. 2023) for alpha and beta diversity analyses.

Alpha diversity was assessed in terms of Chao 1 index (Chao 1987) and Shannon's index (Shannon 1948). Chao 1 Index and Shannon's Index were analyzed with Student's *t*-tests. Beta diversity was assessed by the Bray–Curtis Dissimilarity Index and was analyzed with a Pairwise PERMANOVA (Benjamini-Hochberg False-Discovery Rate adjusted *p* values are reported). Taxonomic data were exported from QIIME2, and relative abundances were computed and analyzed using a nonparametric Mann–Whitney *U* test.

2.14 | Statistical Analysis

A Grubb's Test was used to identify outliers across all datasets prior to subsequent statistical analyses (a total of 164—Figure 2 (30), Figure 3 (45), Figure 4 (35), Figure 5 (23), Figure 6 (0), Figure 7 (14), Figure 8 (14), Figure 9 (3)—were identified). Data were then analyzed with a Fmax test to determine if they failed homogeneity of variance. If data had unequal variance, a Student's *t*-test with Welch's correction (unpaired, two-tailed) was performed. Results are presented as t (degrees of freedom) = t value; $p = p$ value. For two sample tests, data that were normally distributed underwent a Student's *t*-test (unpaired, two-tailed unless otherwise noted). For data that were not normally distributed, the nonparametric equivalent was performed (Mann–Whitney *U* test, all two-tailed with the exception of the olfactory anatomy experiments). For experiments in which data were repeatedly sampled over time (body weight, glucose clearance, metabolic parameters), a 2-way repeated measures ANOVA (2-w RM ANOVA) or a mixed-effects model analysis was applied using time and diet/donor as factors, with Šidák's multiple comparisons test. The F statistic is reported as F (degrees of freedom of numerator, degrees of freedom of denominator) on the associated graph. Normalized fecal DNA concentration was analyzed using a Welch's ANOVA test (W (degrees of freedom of numerator, degrees of freedom of denominator) = W statistic) with Dunnett's T3 multiple comparisons test. Adjusted *p*-values are reported for these analyses. Alpha was set a priori to 0.05. Post hoc significance on graphs are indicated as follows: $*p < 0.05$, $**p < 0.01$, $***p < 0.001$, $****p < 0.0001$. Most graphs were generated and statistical analyses performed in GraphPad Prism software version 10 (Boston, MA, USA). Data points represent the mean ± standard deviation (SD). Violin plots indicate median and 1st and 3rd quartiles, along with individual data points. Sample sizes were not determined a priori. The number of subjects used for the study was based on previous studies from our laboratory (Chelette et al. 2022; Thiebaud et al. 2014). In addition, Kim et al. 2023 utilized similar sample sizes ($N = 5–8$) for fecal microbiota transplantation experiments. Sample sizes are transparent in the figures where individual values are displayed, otherwise (i.e., line graphs), sample size is specified in the figure legend.

3 | Results

Mice were arbitrarily assigned to either control-fat (CF) or moderately high-fat (MHF) chow diets, and fed *ad libitum* for 5 months prior to collection of donor fecal material (Figure 1). Mice were examined for anticipated metabolic changes in response to excess fat consumption.

3.1 | Male Mice Maintained on a Moderately High-Fat Diet Have Increased Body Weight and Impaired Glucose Clearance

Mean weekly body weight in CF- and MHF-treated male mice was significantly different (diet: $p = 0.0004$, 2-w RM ANOVA); post hoc tests indicated the weights of these two groups diverged starting at 10 weeks into dietary maintenance and were retained for the duration of the study (Figure 2a, left: time × diet interaction, $p < 0.0001$). In contrast to male mice, female mice were fairly resistant to the diet in terms of body weight changes (Figure 2a, right). There was no main effect of diet ($p = 0.2272$), and there was a diet × time interaction ($p < 0.0001$). Measurements taken at week 20 indicated that male, but not female, MHF-fed mice weighed significantly more than their CF-fed counterparts (Figure 2b; male: t (17.87) = 4.787; $p = 0.0002$, female: t (16.08) = 1.328; $p = 0.2028$; Student's *t*-test). This increased body weight in male mice attributed to the MHF diet was also associated with an impaired glucose clearance. When challenged with an intraperitoneal glucose tolerance test (IPGTT), selectively male mice maintained on MHF diets showed a main effect of diet (Figure 2c, left (male): $p = 0.0449$, right (female): $p = 0.6795$; 2-w RM ANOVA) in terms of blood glucose. Fasted blood glucose levels (mg/dL) were not different in male (CF: 165.4 ± 20.4 (5), MHF 180.5 ± 17.9 (4); t (7) = 1.160; $p = 0.2841$) or female (CF: 141.6 ± 25.9 (5), MHF: 125.8 ± 18.4 (5); t (8) = 1.113; $p = 0.2982$) mice maintained on modified diets versus control (mean ± SD (*n*), Student's *t*-test). Integrating the area under the curve (iAUC) (Figure 2c, insets) demonstrated that male, but not female, MHF-fed mice had significantly poorer glucose clearance (male: t (7) = 2.548; $p = 0.0382$, female: t (7) = 1.645; $p = 0.1440$; Student's *t*-test).

3.2 | MHF-Fed Mice Have an Increase in Fat Mass, but Not Lean Mass, That Is Independent of Sex

Body composition was measured in an EchoMRI scanner to determine if the elevated body weight in the MHF male group was due to increased lean or fat mass, or a combination of lean and fat mass. Interestingly, both male and female mice exhibited changed body composition when maintained on MHF diets. While lean mass was unchanged (Figure 2d, left: (male) t (20) = 0.5268; $p = 0.6029$; right (female): t (18) = 1.025; $p = 0.3191$; Student's *t*-test), fat mass was significantly elevated in both male and female MHF-fed mice (left (male): t (12.83) = 4.716; $p = 0.0004$; right (female): t (9.516) = 2.903; $p = 0.0166$; Student's *t*-test). Post-mortem adipose tissue dissection was then performed to evaluate if fat was preferentially stored in different regions. For male mice, adipose tissue deposition was elevated across all sources collected, namely intrascapular brown adipose tissue (BAT), gonadal white

adipose tissue (WAT), subcutaneous WAT, and retroperitoneal WAT (Table 1, top: range of $p = 0.0126$ to 0.0450; Student's *t*-test), whereas for female mice, depositions were elevated in each adipose source, but none reached criteria for statistical significance (Table 1, bottom: range of $p = 0.0548$ to 0.5016; Student's *t*-test).

3.3 | Mice Challenged on a MHF Diet Exhibit Metabolic Dysfunction

Mice were next phenotyped in a comprehensive laboratory animal monitoring system (CLAMS) to confirm anticipated changes in metabolism and fuel utilization attributed to the MHF diet

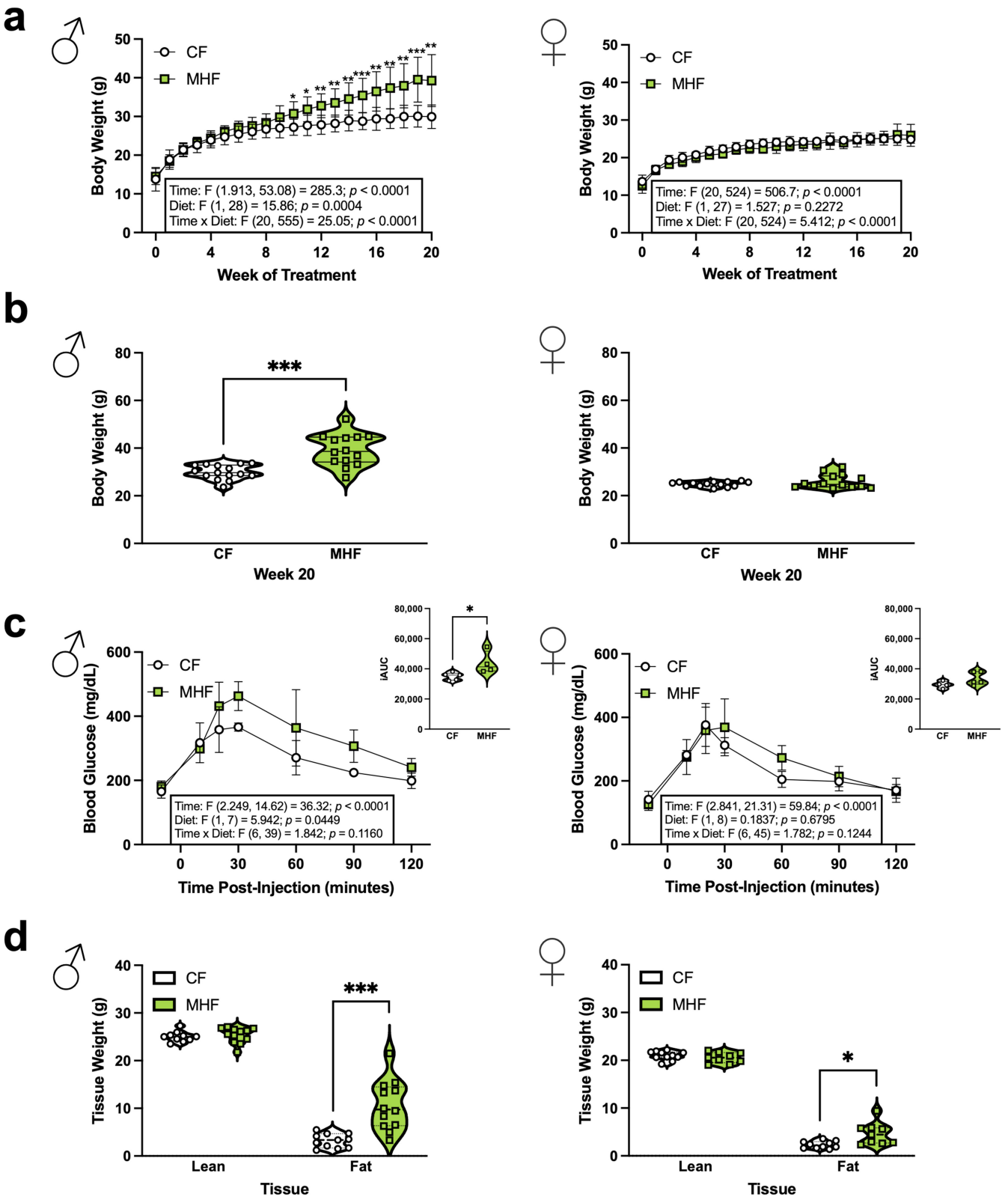

FIGURE 2 | Legend on next page.

FIGURE 2 | Male mice fed a moderately high-fat diet exhibit body weight gain, glucose intolerance, and excess adiposity while female mice do not. (a) Line graph of body weight for male (left) and female (right) mice over 20 weeks of dietary maintenance on control-fat chow (CF) or moderately high-fat chow (MHF). Male: CF $n=15$, MHF $n=15$; Female: CF $n=15$, MHF $n=14$.2-w RM ANOVA. (b) Violin plot of body weight for male (left) and female (right) mice at week 20 of dietary maintenance. Male: CF $n=15$, MHF $n=14$; Female: CF $n=14$, MHF $n=14$. Student's *t*-test. (c) Line graph of blood glucose during an intraperitoneal glucose tolerance test. Male: CF $n=5$, MHF $n=4$; Female: CF $n=5$, MHF $n=5$. Inset: Integrated area under the curve (iAUC) of the line graph. Student's *t*-test. Male: CF $n=5$, MHF $n=4$; Female: CF $n=4$, MHF $n=5$. (d) Violin plot of lean and fat tissue weight in male (left) and female (right) mice maintained on a control-fat chow (CF) or moderately high-fat chow (MHF). Male: Lean CF $n=10$, MHF $n=12$; fat: CF $n=11$, MHF $n=12$; Female: Lean CF $n=11$, MHF $n=9$; fat: CF $n=10$, MHF $n=9$. Student's *t*-test. (a–d) For precise *p* values, please see accompanying text, significantly different $^{*}p<0.05$, $^{**}p<0.01$, $^{***}p<0.001$. Data points represent the mean ± standard deviation (SD). Violin plots indicate median with 1st and 3rd quartiles, along with individual data points.

prior to transfer of their fecal material to recipient mice. Data were plotted for male (Figure 3) and female (Figure 4) mice in hourly bins across a 24-h period to assess oxygen consumption, heat, respiratory exchange ratio (RER), and ambulatory activity (left side of figures), demonstrating mean 12-h dark and light cycle values for each parameter (right side of figures). Male mice exhibited an anticipated drop in oxygen consumption when maintained on the MHF diet (Figure 3a 2-w RM ANOVA) that was attributed to a reduction in the middle of the dark cycle (time × diet interaction, $p=0.0005$) and reflected in a significantly lower 12-h consumption in the dark (Figure 3b, left: dark t (17) = 2.261; $p=0.0371$; right: light t (17) = 0.4177; $p=0.6814$, Student's *t*-test). Female mice exhibited a modest elevation of oxygen consumption when maintained on a MHF diet (Figure 4a, time × diet interaction, dark: $p=0.0237$, light: $p=0.0216$; 2-w RM ANOVA) that appeared to be attributed to a slightly elevated 12-h consumption in the light (Figure 4b, left: dark t (8) = 1.272; $p=0.2391$ right: light t (8) = 2.609; $p=0.0312$; Student's *t*-test). For the male mice, there was a main effect of the MHF diet on heat expenditure in both the dark and light cycle (Figure 3c, diet, dark: $p=0.0367$, light: $p=0.0009$; 2-w RM ANOVA) that was reflected in a significantly elevated 12-h expenditure in the light (Figure 3d, left: dark t (17) = 1.996; $p=0.0622$; right: light t (18) = 3.785; $p=0.0014$; Student's *t*-test). The RER value was also significantly lower in the majority of the dark cycle, extending into the start of the light cycle (Figure 3e, time × diet interaction, dark: $p<0.0001$, light: $p<0.0001$; 2-w RM ANOVA) with a prominent drop during the 12-h dark cycle (Figure 3f, left: dark t (11.15) = 3.150; $p=0.0091$; right: light t (18) = 0.9015; $p=0.3793$, Student's *t*-test) signifying a greater fuel utilization of the fat in the MHF diet for male mice. Modest similar directions were observed in female mice for both heat (Figure 4c,d) and RER (Figure 4e,f), however, the analysis of variance reflected either modest or non-significant *p* values, and the 12-h mean values of these parameters were not different across diet ($p>0.05$; Student's *t*-test). The RER values were significantly lower across the dark cycle for female mice on the MHF diet (time × diet interaction, dark: $p=0.0006$, light: $p=0.0910$; 2-w RM ANOVA), but post hoc analysis did not reflect a specific timepoint within the dark cycle for that drop in ratio ($p>0.05$). Finally, the locomotor activity for both male and female mice did not demonstrate any main effect of diet or have a time × diet interaction during the dark cycle where there was enough ambulatory movement to make the parameter biologically relevant (Figure 3g,h and Figure 4g,h, respectively, $p>0.05$). Although not rigorously examined quantitatively, the pattern of elevated nocturnal activity in both males and females over that in the light cycle does not appear to be affected by the MHF diet.

3.4 | Mice Maintained on a MHF Diet Exhibit Gut Microbiome Dysbiosis

After 5 months of dietary maintenance, the gut microbiome composition of moderately high-fat fed male and female mice had dysbiosis characteristic of fatty diet consumption and diet-induced obesity. Chao 1 and Shannon's Indices were used to estimate alpha diversity. Both male and female mice maintained on a moderately high-fat diet exhibited reduced alpha diversity across both metrics (Figure 5a,c; male: Chao 1: t (24) = 6.699 $p<0.0001$, Shannon: t (24) = 6.013, $p<0.0001$; female: Chao 1: t (22) = 5.901, $p<0.0001$; Shannon: t (14.37) = 6.286, $p<0.0001$; Student's *t*-test). Similarly, dietary groups exhibited distinct beta diversity estimated by Bray–Curtis Dissimilarity Index (Figure 5b,d; male: $F=8.7363$, $p=0.001$, female: $F=12.372$, $p=0.001$; Pairwise PERMANOVA). At the phylum level, male and female mice fed a moderately high-fat diet exhibited elevated relative abundance of Bacillota I and Actinomycetota, reduced relative abundance of Bacteroidota and Campylobacterota A, and unchanged relative abundance of Verrucomicrobiota (Figure 5e–g; Bacillota I male: $U=10$; $p<0.001$, female: $U=36$; $p=0.0246$; Actinomycetota male: $U=23$; $p=0.0010$, female: $U=0$; $p<0.0001$; Bacteroidota male: $U=0$; $p<0.0001$, female: $U=5$; $p<0.0001$; Campylobacterota A male: $U=19$; $p=0.0014$, female: $U=10$; $p=0.0002$; Verrucomicrobiota male: $U=60.50$; $p=0.2571$, female: $U=63$; $p=0.7431$; Mann–Whitney U test). Male mice fed a fatty diet exhibited reduced relative abundance of Bacillota A 368345 abundance, while female mice exhibited no change (male: $U=16$; $p=0.0007$, female: $U=69$; $p=0.6867$, Mann–Whitney U test). At the family level, male and female mice exhibited elevated *Erysipelotrichaceae* and *Bifidobacteriaceae* abundances, and reduced *Lachnospiraceae*, *Muribaculaceae*, *Lactobacillaceae*, and *Bacteroidaceae* abundances (Figure 5h–j, *Erysipelotrichaceae* male: $U=14$; $p=0.0002$, female: $U=0$; $p<0.0001$; *Bifidobacteriaceae* male: $U=13$; $p<0.0001$, female: $U=0$; $p<0.0001$; *Lachnospiraceae* male: $U=5$; $p<0.0001$, female: $U=5$; $p<0.0001$; *Muribaculaceae* male: $U=0$; $p<0.0001$, female: $U=0$; $p<0.0001$; *Lactobacillaceae* male: $U=7$; $p<0.0001$, female: $U=8$; $p<0.0001$; *Bacteroidaceae* male: $U=4$, $p<0.0001$; female: $U=11$, $p<0.0001$, Mann–Whitney U test).

Both male and female mice maintained on the MHF diet exhibited reduced relative abundance of *Muribaculaceae* (phylum Bacteroidota) members *Lepagella muris A, Duncaniella muris, Duncaniella muricolitica, Duncaniella dubosii, CAG-873 sp011959565*, and *Muribaculum intestinale (Lepagella muris A*: male: $U=0$, $p<0.0001$; female: $U=0$, $p<0.0001$; *Duncaniella muris*: male: $U=0$, $p<0.0001$; female: $U=0$, $p<0.0001$;

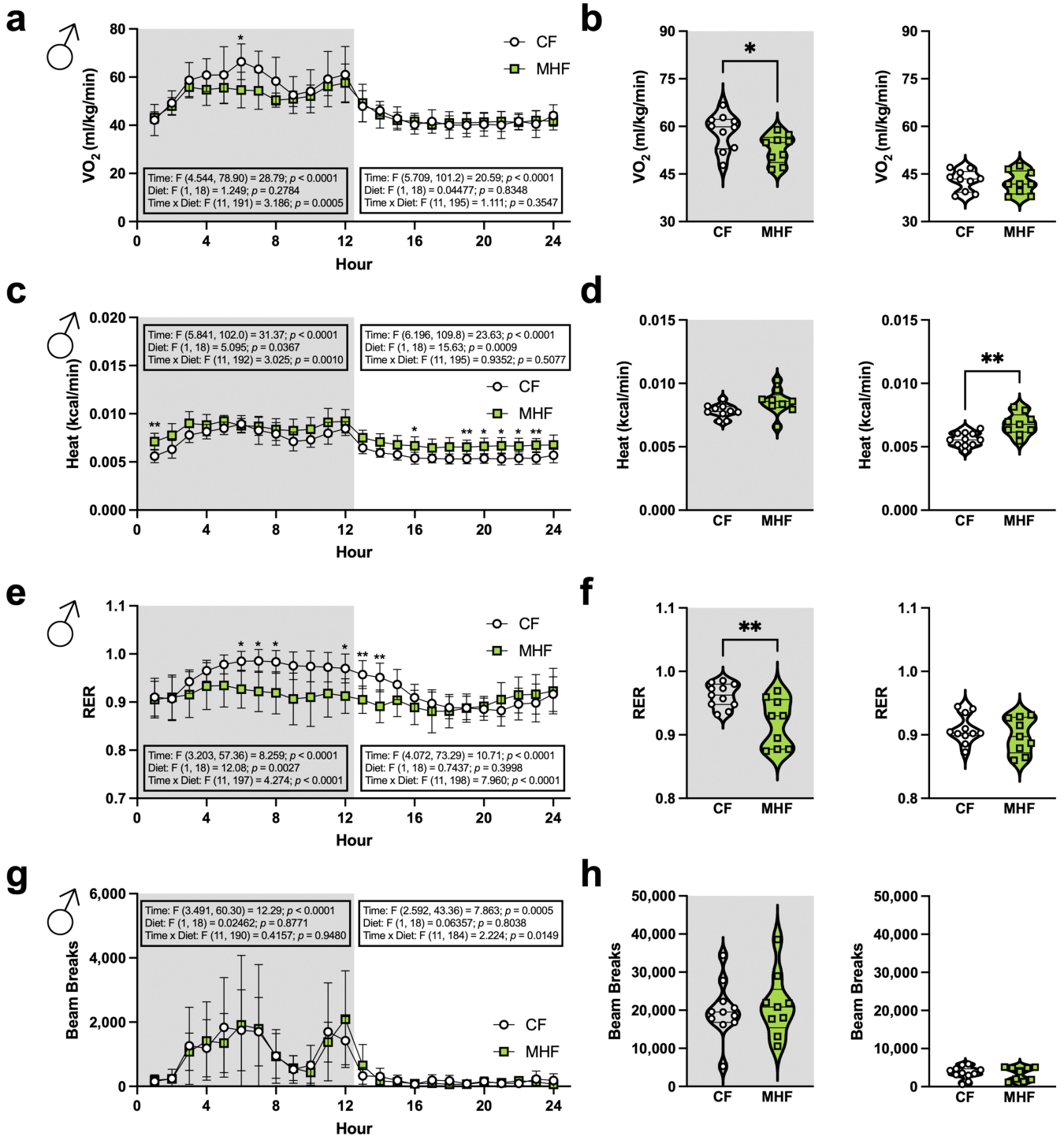

FIGURE 3 | Male mice fed a moderately high-fat diet exhibit metabolic dysfunction. Oxygen consumption (VO_2) (a, b), heat (c, d), respiratory exchange ratio (RER) (e, f), and activity (beam breaks) (g, h) data for male donor mice were assessed by housing mice in metabolic chambers. (a, c, e, g) Line plots represent mean (± SD) physiological parameters for 9–11 mice per CF versus MHF diet treatment collected across 3 days and binned across the 24-h day. 2-w RM ANOVA, Šidák's post hoc test. (b, d, f, h) Violin plots represent median and first/third quartile VO_2, heat, RER, and beam breaks within the dark (left) or light (right) cycle for 9–11 mice per CF vs. MHF diet treatment using similar collection interval but tabulated for a 12-h cycle. Student's *t*-test. (a–h) Shaded and white areas delineate the dark/light cycle, respectively. For precise *p* values, please see accompanying text, significantly different $^*p < 0.05$, $^{**}p < 0.01$.

Duncaniella muricolitica: male: $U = 6.500$, $p < 0.0001$; female: $U = 11$, $p < 0.0001$; *Duncaniella dubosii*: male: $U = 6.500$, $p < 0.0001$; female: $U = 5.500$, $p < 0.0001$; *CAG-873 sp011959565*: male: $U = 0$, $p < 0.0001$; female: $U = 5$, $p < 0.0001$; *Muribaculum intestinale*: male: $U = 0$, $p < 0.0001$; female: $U = 0$, $p < 0.0001$; Mann–Whitney *U* test, Figure S2a–j). Additionally, fat-fed mice also exhibited reduced relative abundance of *Parasutterella muris* and *Prevotella sp902776665*, and elevated relative abundance

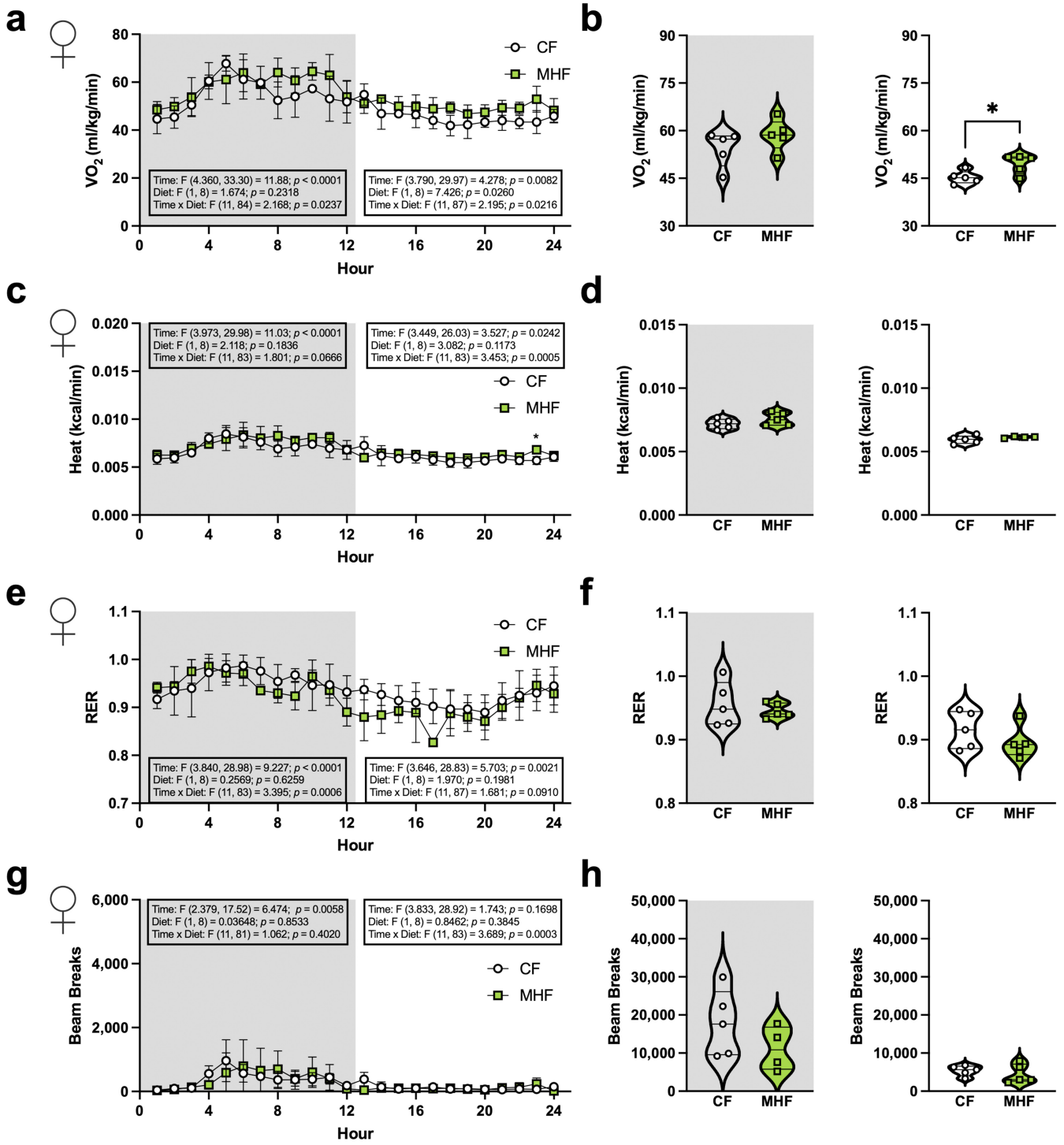

FIGURE 4 | Female mice fed a moderately high-fat diet exhibit metabolic dysfunction. Same experimental design, notations, and statistical analyses as in Figure 3, but for female donors ($n = 5$/group).

of *Bifidobacterium 388775* sp. and *Lactococcus A 346100* sp., compared to their CF-fed counterparts (*Parasutterella muris*: male: $U = 0$, $p < 0.0001$; female: $U = 0$, $p < 0.0001$; *Prevotella sp902776665*: male: $U = 0$, $p < 0.0001$; female: $U = 0$, $p < 0.0001$; *Bifidobacterium 388775* sp.: male: $U = 13$, $p < 0.0001$; female: $U = 0$, $p < 0.0001$; *Lactococcus A 346120* sp.: male: $U = 0$, $p < 0.0001$; female: $U = 0$, $p < 0.0001$; Mann–Whitney U test, Figure S2a–j).

3.5 | Change in Fecal DNA Load and Gut Bacteria Following FMT From Obese Donors

Fecal microbiome transplant (FMT) recipient mice were first treated with antifungal water to prevent fungal bloom upon antibiotic administration. Mice provided *ad libitum* vehicle water or antifungal water consumed water similarly (vehicle 6.2 ± 1.1 mL/day $n = 13$ mice; antifungal 6.9 ± 1.1 mL/day

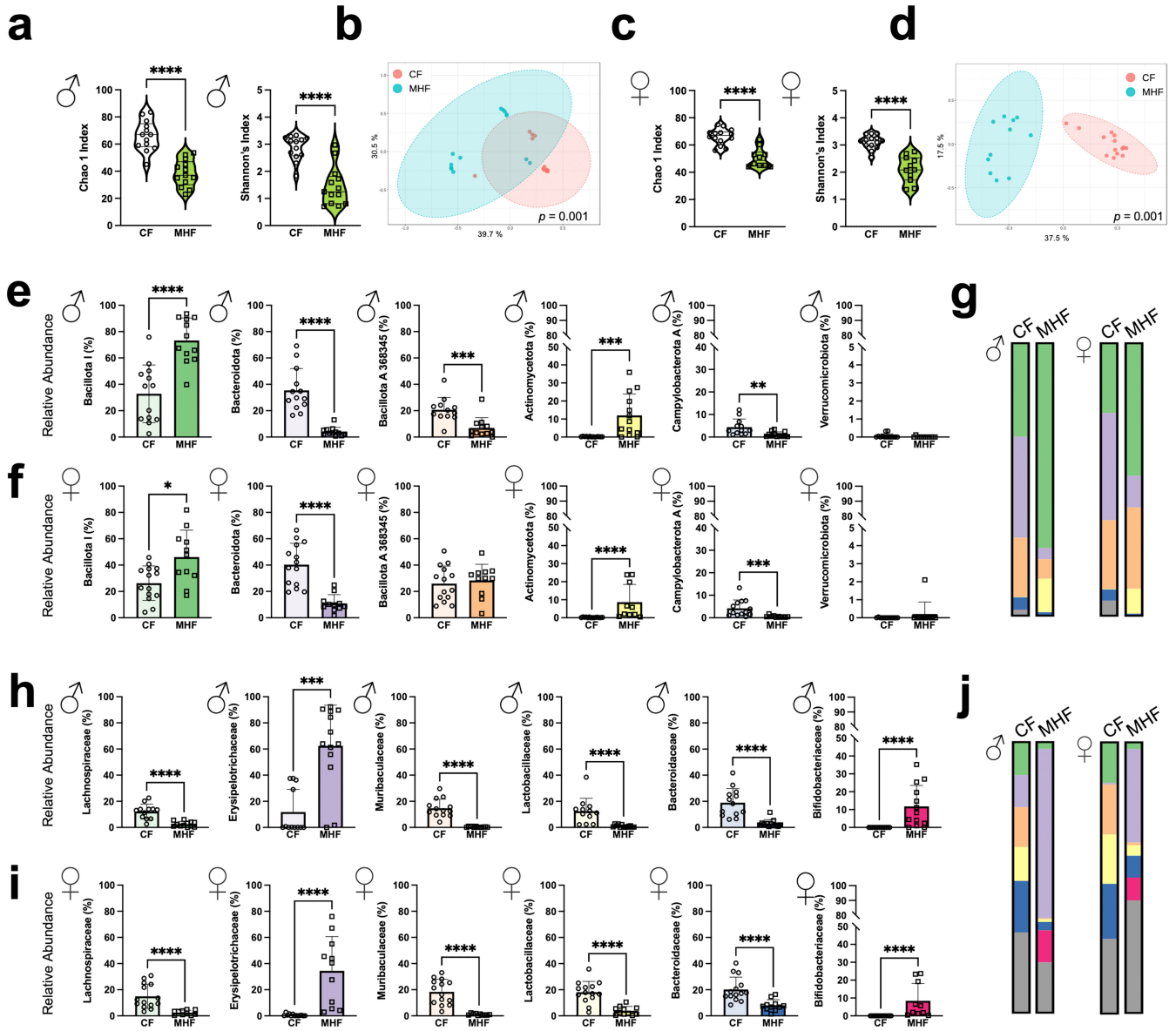

FIGURE 5 | Maintenance on a MHF diet induces gut microbiome dysbiosis. (a) Violin plots reporting alpha diversity reflected in Chao 1 Index and Shannon's Index, and beta diversity reflected in (b) Bray–Curtis Dissimilarity Index Principal Coordinate Analysis plot for male donor mice maintained on CF versus MHF diets. (c,d) Same as (a,b) but for female mice: Chao 1 Index, Shannon's Index, and Bray-Curtis. Bar plots of phylum relative abundance for 6 phyla quantified in e. male and f. female donor mice maintained on CF versus MHF diets. Alpha diversity metrics analyzed by Student's *t*-test, taxonomic relative abundance analyzed by Mann–Whitney *U* test. (g) Mean relative abundance plots for all phyla in (e,f, h–j), same as (e–g) but for family abundance. (a–g) Data points represent the mean ± standard deviation (SD). Violin plots indicate median and 1st and 3rd quartiles, along with individual data points. $n = 10$–14/group. For precise p values, please see accompanying text, significantly different $^{*}p < 0.05$, $^{**}p < 0.01$, $^{***}p < 0.001$, $^{****}p < 0.0001$.

$n = 21$ mice; t (32) = 1.616, $p = 0.1159$, mean ± SD, Student's *t*-test). Treatment with an antibiotic cocktail reduced normalized fecal DNA load compared to that in untreated CF-fed mice (Figure 6, W (2.000, 16.69) = 249.8; $p < 0.0001$; Untreated versus Abx treated $p < 0.0001$, Welch's ANOVA). These data indicated a significant drop in fecal DNA concentration following antibiotic depletion and elevation of DNA concentration following FMT. Body weight was monitored throughout antifungal, antibiotic, and donor material administration to monitor animal health (mean minimum body weight: 95.0% of pre-treatment body weight ± 5.7% (SD)).

In contrast to mice maintained on modified diets, FMT-MHF recipient animals exhibited no reduction in alpha diversity (male: Chao 1 Index: t (6) = 1.904, $p = 0.1055$, Shannon's Index: t (7) = 0.7416, $p = 0.4825$; female: Chao 1 Index: t (12) = 0.5567, $p = 0.5880$; Shannon's Index: t (12) = 1.060, $p = 0.3099$, Student's *t*–test) or distinct beta diversity (Bray–Curtis Dissimilarity Index, male $F = 1.2815$, $p = 0.286$, female $F = 1.2259$, $p = 0.245$) (Figure 7a–d). At the phylum level, transplantation did not cause any changes in relative abundance (Figure 7e–g, Bacillota I: male: $U = 5$; $p = 0.2857$, female: $U = 23$; $p = 0.9015$; Bacteroidota: male: $U = 6$; $p = 0.4127$, female: $U = 16$; $p = 0.3176$;

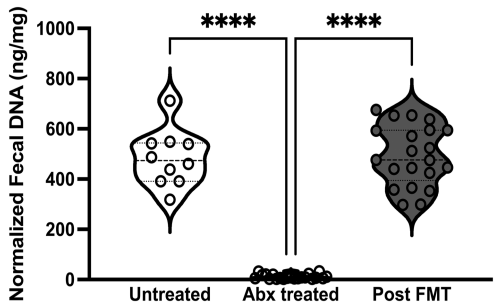

FIGURE 6 | Treatment with an antibiotic cocktail reduces fecal DNA load, which is reversed by fecal microbiome transplantation. Violin plot of normalized (to fecal input weight) fecal DNA extracted from untreated recipient mice (untreated $n=10$), antibiotic-treated recipient mice (Abx treated $n=21$), and recipient mice post-fecal microbiome transplantation (Post FMT $n=21$). Welch's ANOVA. Violin plots indicate median and 1st and 3rd quartiles, along with individual data points. For precise p values, please see accompanying text, significantly different ****$p<0.0001$.

Bacillota A 368345: male: $U=8$; $p=0.7302$, female: $U=18$; $p=0.7308$; Actinomycetota: male: $U=4$; $p=0.1905$, female: $U=15$; $p=0.6991$; Campylobacterota A: male: $U=6$; $p=0.4127$, female: $U=10.50$; $p=0.0769$; Verrucomicrobiota: male: $U=2$; $p=0.2286$, female: $U=10$; $p=0.2338$; Mann–Whitney U test). At the family level, however, male FMT-MHF mice exhibited increased *Erysipelotrichaceae* relative abundance and decreased *Lactobacillaceae* relative abundance, similar to MHF-fed donor animals (Figure 7h–j, *Erysipelotrichaceae* $U=0$; $p=0.0357$; *Lactobacillaceae* $U=0$; $p=0.0286$, Mann–Whitney U test). No other differences in relative abundance were observed at the family level (*Lachnospiraceae* male: U = 8, $p=0.7302$, female: $U=20$; $p=0.9452$; *Erysipelotrichaceae* female: $U=19$; $p=0.5350$; *Muribaculaceae* male: $U=7$; $p=0.5556$, female: $U=16$; $p=0.3176$; *Lactobacillaceae* female: $U=20$; $p=0.6200$; *Bacteroidaceae* male: $U=7$; $p=0.5556$, female: $U=19$; $p=0.5350$; *Bifidobacteriaceae* male: $U=1.500$; $p=0.1071$, female: $U=15$; $p=0.6991$, Mann–Whitney U test). Despite no change of total *Muribaculaceae* relative abundance, FMT-MHF male recipient mice exhibited a reduction in relative abundance of *Duncaniella muris* compared to their FMT-CF counterparts ($U=0$; $p=0.0286$, Mann–Whitney U test; Figure S3a–j).

3.6 | Lack of Change in Body Weight, Glucose Clearance, or Body Composition for Recipient Mice Following FMT From Obese Donors

Following FMT of fecal homogenate from CF- and MHF-maintained donors, body weight was monitored biweekly in male and female recipient mice and is plotted as raw body weight (Figure 8a) or percent change from pretreatment baseline (Figure 8b).

Mice that received fecal transplantation from MHF-maintained donors (FMT-MHF) exhibited no difference in body weight compared to that of their FMT-CF counterparts (Figure 8a, no main effect of donor or donor × time interaction, $p>0.05$, 2-w RM ANOVA). The same was true for data normalized as percent change from pretreatment baseline (Figure 8b, no main effect of donor or donor × time interaction, $p>0.05$, 2-w RM ANOVA). When challenged with an IPGTT, neither male nor female recipient mice receiving FMT from MHF-maintained donors showed main effects of donor or a donor × time interaction (Figure 8c, $p>0.05$, 2-w RM ANOVA) in terms of blood glucose. Fasted blood glucose levels (mg/dL) were not different in male (CF: 120.5 ± 14.8 (4), MHF: 107.8 ± 6.5 (5); t (7) = 1.743; $p=0.1249$) or female (CF: 111.0 ± 10.3 (7), MHF: 112.6 ± 16.9 (7); t (12) = 0.2096; $p=0.8375$) mice receiving fecal material from CF- or MHF-fed donors (mean ± SD (n), Student's t-test). Integrating the area under the curve (iAUC) (Figure 8c, insets) also showed no significant change in glucose clearance for recipients receiving FMT from MHF-fed donor mice (male t (7) = 0.1620; $p=0.8759$, female t (12) = 0.3569; $p=0.7274$; Student's t-test). Body composition analysis revealed no difference in total lean or fat mass for recipient mice receiving FMT from MHF-fed donor mice (Figure 8d, $p>0.05$, Student's t-test) for either sex. Post-mortem tissue collection revealed a significant reduction in subcutaneous WAT weight in recipient male mice receiving FMT from MHF-fed donor mice ($p=0.0334$), with no difference in any other adipose tissue depot weights or organ weights (Table 2, Student's t-test). For female mice, there was a significant elevation in retroperitoneal WAT weight in recipient mice receiving FMT from MHF-fed mice ($p=0.0185$), with no difference in other adipose tissue depot weights or organ weights (Table 2, Student's t-test).

3.7 | Lack of Olfactory Glomerular Changes Following FMT From Obese Donors

Following fix-perfusion, olfactory bulbs were dissected and whole-mount images were taken to measure glomerular area of the lateral Olfr160 glomerulus (Figure 9a). Glomerular area was measured, and there was no significant reduction in glomerular area in FMT-MHF male or female recipient mice (Figure 9b left (male): $U=37$; $p=0.4143$, right (female): $U=70$; $p=0.1627$; Mann–Whitney U test, one-tailed). After olfactory bulbs were optically cleared, volume measurements of both lateral and medial Olfr160 glomeruli were collected (Figure 9c,e). There was also no significant reduction in lateral or medial glomerular volume in mice that had received transplants from MHF donors (Figure 9d,f, lateral: left (male) $U=23$; $p=0.1179$, right (female): $U=73$; $p=0.4050$; medial: left (male): $U=33$; $p=0.2863$, right (female): $U=66$; $p=0.1872$ Mann–Whitney U test, one-tailed).

4 | Discussion

To our knowledge, this is the first study to perform fecal microbiome transplantation (FMT) from control-fat (CF) or moderately high-fat (MHF) fed mice with the intent to separate olfactory structural changes attributed to consumption of excess dietary fat from those associated with the gut microbiome following diet-induced obesity (DIO). MHF-fed mice exhibited body weight gain, glucose intolerance, increased fat mass and adiposity, and metabolic dysfunction that was sexually dimorphic—induction of diet-induced obesity (DIO) and related metabolic dysfunction was observed for male mice, while female mice exhibited a resistance to DIO. Despite this resistance observed in female mice, both sexes of MHF-fed mice exhibited largely similar gut microbiome

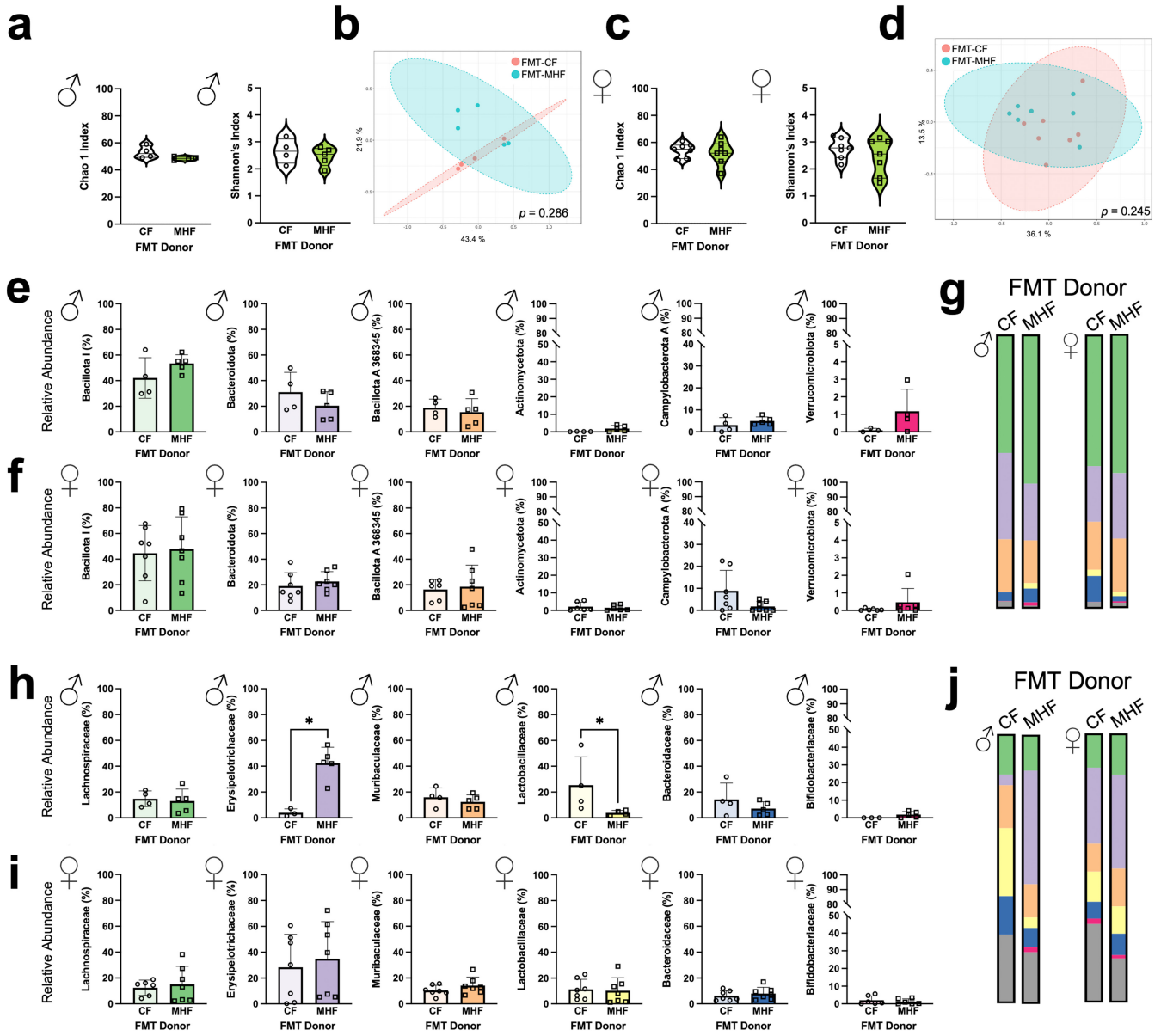

FIGURE 7 | The gut microbiome of male FMT recipient mice shows signatures of donor mice, while that of female mice does not. Same experimental design, notations, and statistical analyses as in Figure 5, but for recipient mice receiving FMT from CF- versus MHF-fed donors. Data points represent the mean ± standard deviation (SD). Violin plots indicate median and 1st and 3rd quartiles, along with individual data points. $n = 3–7$/group. For precise p values, please see accompanying text, significantly different $^*p < 0.05$.

dysbiosis. Even given the reduced alpha diversity, dissimilar beta diversity, and similar phyla- and family-level changes in both sexes following maintenance on the MHF diet, two family-level microbiome changes were observed in male recipient mice. Male FMT-MHF recipient mice also exhibited reduced relative abundance of *Duncaniella muris*, a member of the *Muribaculaceae* family. *Muribaculaceae* have been associated with fiber metabolism and short-chain fatty acid production, and have reported negative associations with type 2 *diabetes mellitus* and obesity (reviewed by (Zhu et al. 2024)). This reduction in FMT-MHF male mice indicates a dietary effect on the gut microbiome that was successfully transmitted from the fecal material of fat-fed animals to male recipient mice. Therefore, it appears that oral consumption of excess fat evokes microbiome dysbiosis, but that elevation of *Erysipelotrichaceae*, reduction in *Lactobacillaceae*, and reduction in *Duncaniella muris* were not sufficient for reduction of olfactory glomerular size, which importantly mediates coding of olfactory information and is reduced following DIO (Chelette et al. 2022; Thiebaud et al. 2014).

We observed elevated relative abundance of *Bifidobacteriaceae* in both male and female mice maintained on the moderately high-fat diet. *Bifidobacterium* species have been associated with milk oligosaccharides (Laursen 2021; Laursen et al. 2021; Laursen and Roager 2023). The moderately high-fat diet utilized in our study contains milk fats, which likely drives the elevation of *Bifidobacteriaceae* abundance observed in fat-fed animals.

A limitation of our study is the large time window of fecal sample collection. The gut microbiome is known to exhibit circadian

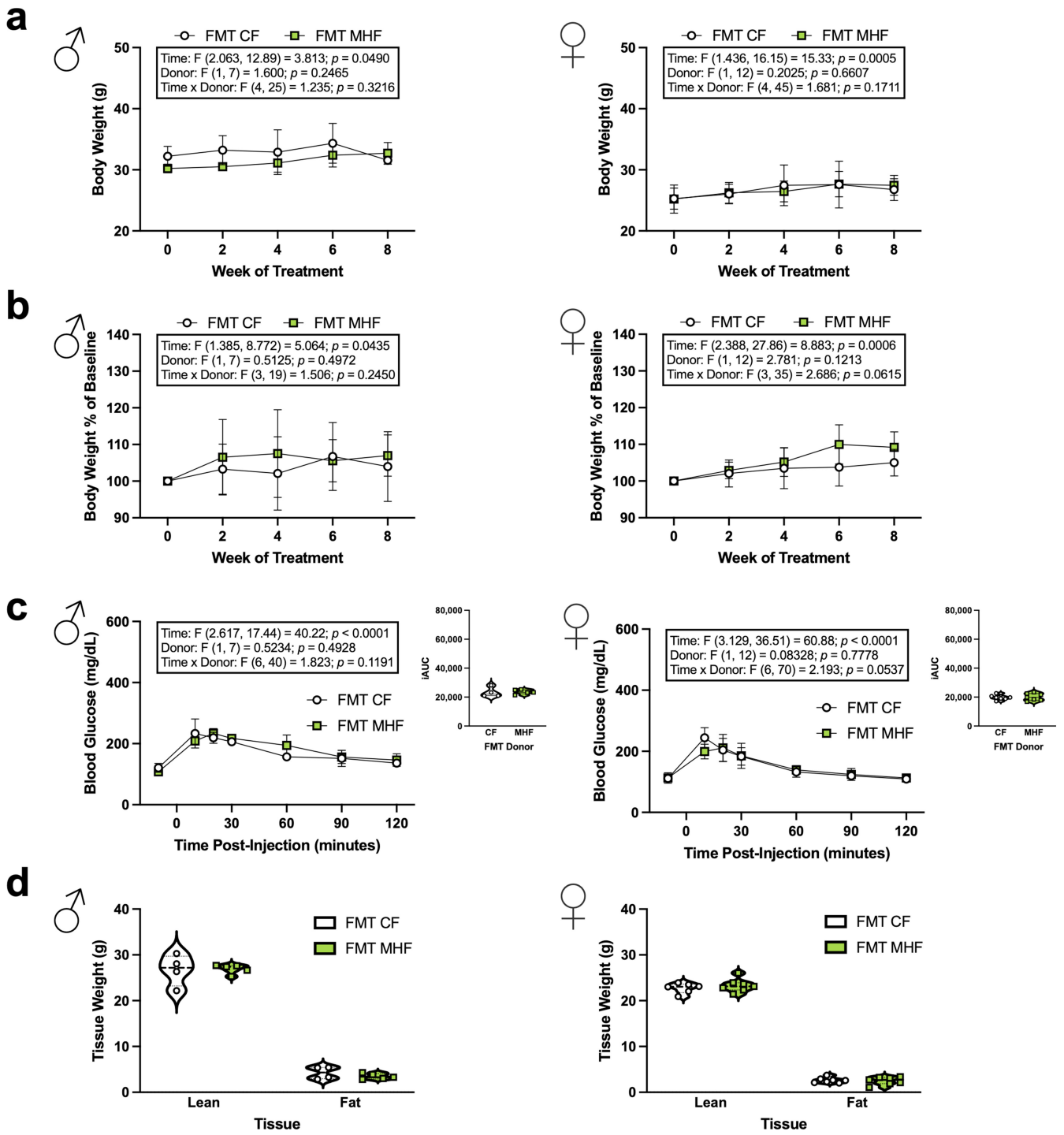

FIGURE 8 | Lack of changes in body weight, glucose clearance, and body composition in recipient mice following FMT from obese donors. (a) Line graph of body weight for male (left) and female (right) mice over 8 weeks post fecal microbiome transplant from donors maintained on control-fat chow (FMT-CF) or moderately high-fat chow (FMT-MHF). Data represent 4–7 mice per FMT treatment. (b) Same as in (a) but converted to percent change from baseline weight week 0 post-FMT. (c) Line graph of blood glucose during an intraperitoneal glucose tolerance test. Data represent 4–7 mice per FMT treatment. Inset: Integrated area under the curve (iAUC) of the line graph. Male: CF $n = 4$, MHF $n = 5$, Female CF $n = 7$, MHF $n = 7$. (d) Violin plot of lean and fat tissue weight in male (left) and female (right) mice. Male: Lean CF $n = 4$, MHF $n = 5$, fat CF $n = 4$, MHF $n = 5$, Female: Lean CF $n = 7$, MHF $n = 7$, fat CF $n = 7$, MHF $n = 7$. (a–c) = 2-w RM ANOVA, $p > 0.05$; (c) inset, (d) = Student's t-test; male lean mass with Welch's correction, $p > 0.05$. Data points represent the mean ± standard deviation (SD). Violin plots indicate median and 1st and 3rd quartiles, along with individual data points. $n = 4$–7/group.

rhythms (Thaiss et al. 2014, 2016; Tofani et al. 2025) that could increase variability within our study. To minimize the effects of fecal collection time across treatment groups, fecal samples were collected across diet/donor groups and sex at a single time. It is important to note that although we describe the study diets in terms of dietary fat content (control-fat, moderately high-fat), the

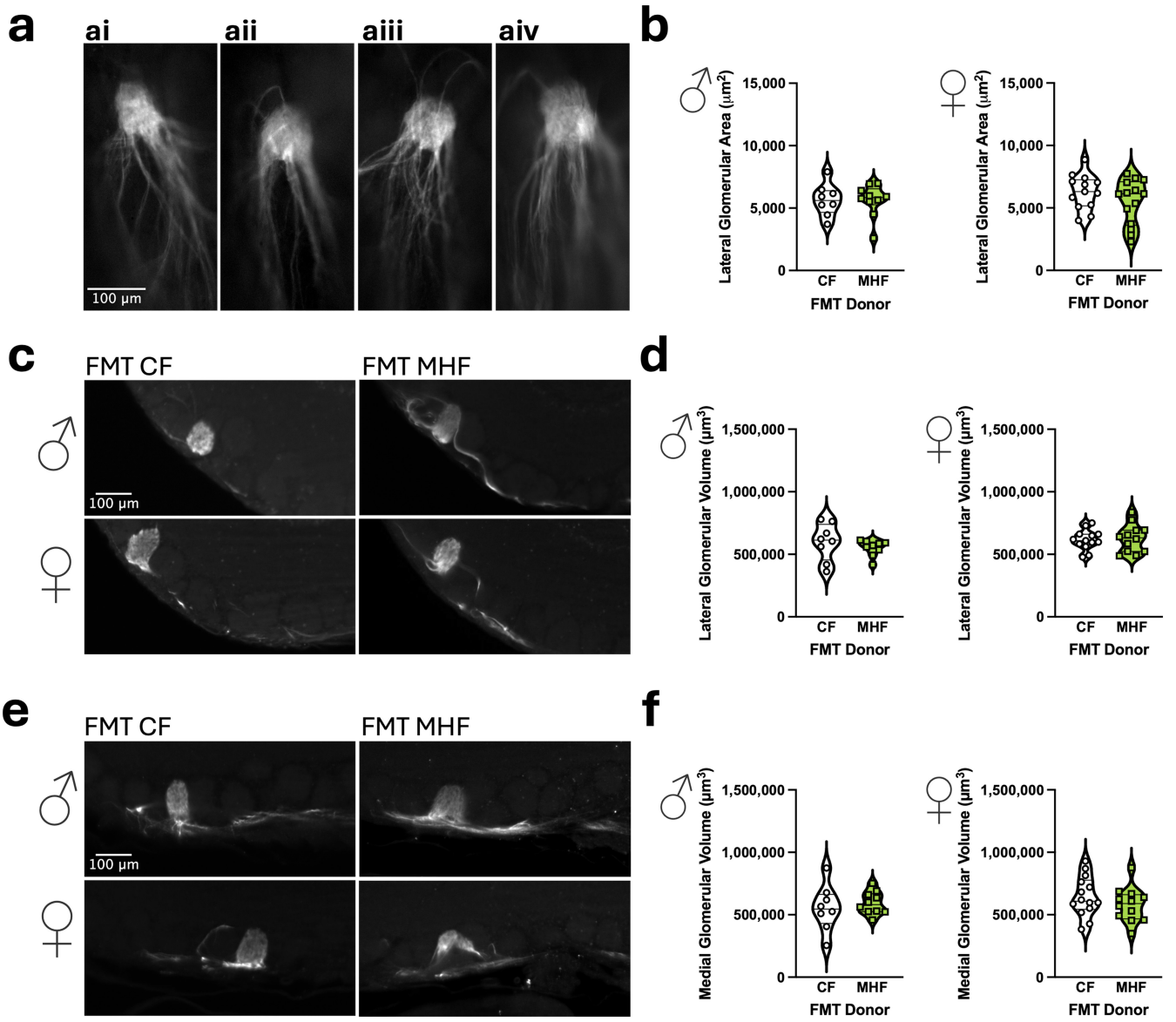

FIGURE 9 | Olfr160 glomerular area and volume are not altered in recipient mice following FMT from obese donors. (a) Representative whole-mount images of lateral Olfr160 glomeruli in male (ai CF, aii MHF) and female (aiii CF, aiv MHF) mice following FMT from CF- versus MHF-fed donors. (b) Violin plot of lateral glomerular area in male (left) and female (right) mice. Each data point is a single lateral glomerulus. Male CF $n = 8$, MHF $n = 10$, Female CF $n = 13$, MHF $n = 14$, Mann–Whitney U test. (c) Representative cross-sectional images of lateral Olfr160 glomeruli in male (top) and female (bottom) mice following FMT from CF- vs. MHF-fed donors. (d) Violin plot of lateral glomerular volume in male (left) and female (right) recipient mice. Male CF $n = 8$, MHF $n = 9$, Female CF $n = 13$, MHF $n = 12$. Each data point is a single lateral glomerulus. (e,f) Same statistical analyses and sample size as (c,d) but for the medial glomeruli. Male CF $n = 8$, MHF $n = 10$, Female CF $n = 14$, MHF $n = 12$, Mann–Whitney U test. Violin plots indicate median and 1st and 3rd quartiles, along with individual data points.

MHF diet could also be characterized as a "lower protein" diet (18% in CF chow, 12% in MHF chow). Therefore, our observed metabolic and microbial effects of diet could be interpreted as a combination of the elevation in fat and reduction in protein. The 6% change in protein may be a less driver than the 18% change in fat (3×). Future studies would benefit from a custom diet that varies in a single macronutrient composition to elucidate the effects of elevated dietary fat and reduced dietary protein, separately.

We have previously demonstrated that DIO or consumption of excess dietary fat in lean mice results in a reduction of the number of Olfr160 olfactory sensory neurons (OSNs) and their axonal projections to Olfr160 glomeruli (Chelette et al. 2022; Thiebaud et al. 2014). DIO also results in a reduction of neuronal activity within the olfactory bulb as determined by decreased immediate early gene activation (Fardone et al. 2019) and by a reduction in action potential firing frequency of the predominant output neurons (Fadool et al. 2011). It should be noted that DIO, isocaloric feeding, and FMT from obese donors all result in inflammation (Al Bander et al. 2020; Chelette et al. 2022), and yet, FMT from DIO donors was ineffective in reducing glomerular volumes in the recipient mice. We hypothesize that retention of normal axon projections and associated glomerular volumes for olfactory information coding may require a coordination of several systems including the immune system, glucose homeostasis, and gut health—and full loss of circuitry structure is not seen unless

TABLE 1 | Male mice fed a moderately high-fat diet display elevated adipose deposition across several regions, while female mice do not.

		Weight (g)		
	Tissue	CF	MHF	Results
Male				
$n = 6, 6$	BAT	0.10 ± 0.02	0.22 ± 0.09	t (5.390) = 3.449; p = 0.0162*
$n = 6, 7$	Gonadal WAT	0.44 ± 0.22	1.42 ± 0.86	t (6.880) = 2.918; p = 0.0228*
$n = 6, 6$	Subcutaneous WAT	0.17 ± 0.06	0.42 ± 0.23	t (5.721) = 2.557; p = 0.0450*
$n = 6, 7$	Retroperitoneal WAT	0.13 ± 0.05	0.44 ± 0.24	t (6.667) = 3.382; p = 0.0126*
Female				
$n = 6, 4$	BAT	0.08 ± 0.01	0.11 ± 0.03	t (8) = 2.247; p = 0.0548
$n = 6, 4$	Gonadal WAT	0.19 ± 0.09	0.23 ± 0.08	t (8) = 0.7036; p = 0.5016
$n = 6, 4$	Subcutaneous WAT	0.11 ± 0.04	0.23 ± 0.16	t (3.269) = 1.501; p = 0.2231
$n = 6, 4$	Retroperitoneal WAT	0.06 ± 0.04	0.14 ± 0.10	t (3.513) = 1.505; p = 0.2164

Note: Post-mortem adipose tissue analysis was performed. Data are presented as mean ± SD for male and female mice. Data were analyzed by Student's t-test. Data presented as t (df) = t value.
Abbreviations: BAT, brown adipose tissue; WAT, white adipose tissue.
*Significantly different ($p < 0.05$).

TABLE 2 | MHF recipient mice do not display elevated weights of adipose deposits or other organs.

		Weight (g)		
	Tissue	FMT CF	FMT MHF	Results
Male				
$n = 3, 5$	BAT	0.07 ± 0.00	0.07 ± 0.01	t (4.000) = 0.6667; p = 0.5415
$n = 4, 5$	Gonadal WAT	0.19 ± 0.04	0.16 ± 0.05	t (7) = 1.044; p = 0.3312
$n = 4, 5$	Subcutaneous WAT	0.10 ± 0.01	0.07 ± 0.01	t (7) = 2.641; p = 0.0334*
$n = 4, 5$	Retroperitoneal WAT	0.07 ± 0.04	0.04 ± 0.02	t (7) = 1.544; p = 0.1665
$n = 3, 5$	Mesenteric WAT	0.18 ± 0.03	0.19 ± 0.05	t (6) = 0.3139; p = 0.7642
$n = 4, 5$	Liver	0.81 ± 0.38	0.81 ± 0.32	t (7) = 0.008549; p = 0.9934
$n = 4, 5$	Spleen	0.13 ± 0.05	0.12 ± 0.02	t (7) = 0.6206; p = 0.5545
Female				
$n = 7, 7$	BAT	0.07 ± 0.02	0.09 ± 0.03	t (12) = 1.646; p = 0.1256
$n = 7, 7$	Gonadal WAT	0.22 ± 0.06	0.34 ± 0.17	t (7.656) = 1.825; p = 0.1071
$n = 7, 7$	Subcutaneous WAT	0.09 ± 0.03	0.12 ± 0.06	t (12) = 1.396; p = 0.1880
$n = 7, 7$	Retroperitoneal WAT	0.06 ± 0.02	0.10 ± 0.03	t (12) = 2.722; p = 0.0185*
$n = 7, 6$	Mesenteric WAT	0.24 ± 0.08	0.29 ± 0.07	t (11) = 1.063; p = 0.3107
$n = 7, 7$	Liver	1.20 ± 0.54	1.09 ± 0.52	t (12) = 0.3900; p = 0.7033
$n = 7, 7$	Spleen	0.16 ± 0.07	0.12 ± 0.02	t (6.874) = 1.499; p = 0.1784

Note: Post-mortem adipose tissue and organ analyses were performed. Data are presented as mean ± SD for male and female mice. Data were analyzed by Student's t-test. Data presented as t (df) = t value.
Abbreviations: BAT, brown adipose tissue; WAT, white adipose tissue.
*Significantly different ($p < 0.05$).

there is disruption in more than one system. Changes in solely gut microbiota were not sufficient to alter the anatomical structures. With 20 weeks of chronic fatty-diet maintenance, excess dietary fat could also be associated with lipotoxicity that could affect olfactory synaptic development and maintenance, but is absent in FMT-MHF recipient animals consuming control-fat chow (Bianchettin et al. 2025). Another interpretation is that our previous challenge with DIO occurred upon weaning age, whereas the FMT was performed as an adult mouse. It is possible that the developmental critical window surrounding the

transition from lactation to solid foods that occurs around weaning (Al Nabhani et al. 2019; Ardeshir et al. 2024) could provide a greater deal of plasticity of these circuits exposed to MHF in donor mice. Our recipient mice were 6 months of age when they received altered microbiota by FMT, a period during which the olfactory glomerular maps may be less plastic. Aging also causes a loss of up to 60% of olfactory sensory neurons (OSNs) in comparison to the abundance in early postnatal stages (Cavallin et al. 2010; Costanzo and Kobayashi 2010), and the effects of obesity on these structures in relation to potential injury mechanisms, inflammation, or cell turnover changes may be altered with age (Kobayashi et al. 2025; Mobley et al. 2014).

Functional differences exist between medial and lateral glomeruli. In vivo multielectrode experiments have revealed different odor-evoked response latencies in the medial vs. lateral OB (Zhou and Belluscio 2012), and calcium imaging experiments have reported greater respiration-locked calcium fluctuations in post-synaptic cells of the medial glomeruli compared to that of the lateral glomeruli (Sato et al. 2020). Previously, we observed that DIO differentially affects functional activation of the medial vs. the lateral glomerulus (Fardone et al. 2019), thus, we anticipated that the lateral glomeruli might have greater volume changes than that of the medial glomeruli following FMT in recipient mice. We did not see this to be the case. There was no difference in how medial vs. lateral glomeruli responded to FMT (neither were affected by transfer of MHF-diet donor fecal material). While our hypothesis was rejected, and we did not see a reduction in glomerular volume, male recipient mice had a trend for smaller lateral glomeruli ($p = 0.1179$), and female recipient mice had a trend for smaller medial glomeruli ($p = 0.1872$), albeit not reaching statistical significance.

We and others have demonstrated that early-life sensory experiences may influence glomerular plasticity, and not just dietary manipulation. For example, chronic prenatal and early postnatal exposure to high-affinity Olfr160 ligands—such as methyl salicylate and isopropyl tiglate—have been shown to increase cross-sectional glomerular area and volume; these changes are often accompanied by the appearance of supernumerary glomeruli and an increased number of glomeruli-associated mitral and tufted cells (Liu, Savya, and Urban 2016; Todrank et al. 2011; Valle-Leija et al. 2012). When these same experiments are performed on 4–6 month to 1-year old mice, the opposite occurs—there is a decrease in number of olfactory sensory neurons (OSNs) and glomeruli-associated mitral and tufted cells following daily odor exposure to acetophenone, peppermint or citralva (Cavallin et al. 2010; Johnson et al. 2013) that would be correlated to smaller glomerular volumes for the Olfr160 glomerulus (see (Bressel et al. 2016)). Moreover, this loss of odor-enrichment-induced OSN abundance was prevented in Kv1.3−/− mice, suggesting that voltage-gated activity of mitral cells is also important for OSN plasticity and glomerular volume (also noted in (Biju et al. 2008)). In our experiments, FMT was performed in adult mice (~6 months old) and the transplantation did not evoke prediabetes, glucose resistance, or body composition changes. The timing of dietary intervention is therefore judged as critical for translating OSN loss into reduced glomerular volume, but it is not the only factor that modulates OSN abundance or glomerular size. Taken together, these findings indicate that while diet composition can affect the olfactory system, the extent of its impact on Olfr160 area and volume appears to be additionally driven by aging, voltage-gated activity, and early life developmental changes.

The observation that female mice lacked a traditional obesogenic phenotype following maintenance on a MHF diet has been noted previously (Chelette et al. 2022). Moreover, it has been shown that females introduced to a fatty diet at a young age are more resistant to DIO, and this resistance was lost when a fatty diet was administered in aged female mice (Salinero et al. 2018). Despite these resistance changes for female mice that were administered MHF diet upon weaning, a previous study (Loeven et al. 2025) and this current study do not observe broad sexual dimorphism in the microbiota dysbiosis at either the phyla or family level for our male and female mice treated chronically with MHF diet *ad libitum*. Following the FMT, male recipient mice that received fecal material from MHF-treated donors exhibited elevated relative abundance of *Erysipelotrichaceae* and reduced abundance of *Lactobacillaceae*. These shifts are associated with obesity but are not associated with changes to an obesogenic phenotype in our study (either body weight, glucose tolerance, body composition, or olfactory anatomy). Because we did not observe an obesogenic phenotype following FMT, this could also be interpreted as a difference in severity of the length of treatment—8 weeks of gut microbiome transplantation vs. that of 20 weeks of fatty-diet maintenance, although other studies have certainly reported changes in taxonomic distribution, neurological and behavioral dysfunctions, and synaptic changes in as short as 3–5 weeks following FMT (Crain et al. 2025; Kim et al. 2023; Klug et al. 2025) with and without obesity.

Future studies could investigate changes in olfactory behavior or reduction in electroolfactogram amplitude following FMT from obese donors that would reflect loss of OSNs or axonal density and associated functional changes not detected in glomerular volume measurements. Likewise, it would be informative if FMT from obese donors was performed during the developmental window surrounding weaning to understand any contribution of a critical period reflected in anatomical, structural, or functional changes attributed to DIO and associated gut microbiome dysbiosis.

Author Contributions

Ashley M. Loeven: conceptualization, investigation, funding acquisition, writing – original draft, methodology, validation, visualization, writing – review and editing, formal analysis, data curation. **Franklin A. Pacheco:** investigation, writing – original draft, writing – review and editing, formal analysis. **Amber N. Brown:** investigation, writing – review and editing, methodology, formal analysis. **Debra Ann Fadool:** conceptualization, funding acquisition, writing – original draft, validation, visualization, writing – review and editing, formal analysis, supervision, resources, project administration, data curation.

Acknowledgments

This work was funded by T32 DC000044, F31 DC019867, and R01 DK133464 from the National Institutes of Health (NIH), and a generous endowment from the Robinson Family and the Tallahassee Memorial Hospital. We would like to thank Jaime White-James for staff assistance

with mouse husbandry and routine maintenance. We would like to thank a number of undergraduate directed individual study students and their supervisors (Jenna Claydon, Claudia Silver, Joshua Cazorla, Caroline Bishop, Camilla May, and Martina Compagno) for their arduous help in animal husbandry. We would like to thank Dr. Claire de La Serre (Colorado State University—College of Veterinary Medicine and Biomedical Sciences) for her advice in experimental design and data analyses.

Funding

This work was supported by the Robinson Family and the Tallahassee Memorial Hospital. National Institutes of Health (F31 DC019867, R01 DK133464, T32 DC000044).

Conflicts of Interest

The authors declare no conflicts of interest.

Data Availability Statement

All data are readily available through contacting the communicating author. Excess fecal material is also available for experiments upon request, with shipping costs borne by the requester.

Peer Review

The peer review history for this article is available at https://www.webofscience.com/api/gateway/wos/peer-review/10.1111/jnc.70396.

References

Al Bander, Z., M. D. Nitert, A. Mousa, and N. Naderpoor. 2020. "The Gut Microbiota and Inflammation: An Overview." *International Journal of Environmental Research and Public Health* 17, no. 20: 7618. https://doi.org/10.3390/ijerph17207618.

Al Nabhani, Z., S. Dulauroy, R. Marques, et al. 2019. "A Weaning Reaction to Microbiota Is Required for Resistance to Immunopathologies in the Adult." *Immunity* 50, no. 5: 1276–1288.e5. https://doi.org/10.1016/j.immuni.2019.02.014.

Ardeshir, A., T. Gensollen, M. Zeng, Z. Al Nabhani, and R. Blumberg. 2024. "Editorial: The Early Life Window of Opportunity: Role of the Microbiome on Immune System Imprinting." *Frontiers in Immunology* 15: 1417060. https://doi.org/10.3389/fimmu.2024.1417060.

Bäckhed, F., H. Ding, T. Wang, et al. 2004. "The Gut Microbiota as an Environmental Factor That Regulates Fat Storage." *Proceedings of the National Academy of Sciences* 101, no. 44: 15718–15723. https://doi.org/10.1073/pnas.0407076101.

Bianchettin, R. G., B. J. Gawey, A. J. Acosta, et al. 2025. "Clinical Assessment of People With Obesity: Focus on Adiposity-Related Multimorbidity." *Mayo Clinic Proceedings* 100, no. 6: 1005–1029. https://doi.org/10.1016/j.mayocp.2025.02.021.

Biju, K. C., D. R. Marks, T. G. Mast, and D. A. Fadool. 2008. "Deletion of Voltage-Gated Channel Affects Glomerular Refinement and Odorant Receptor Expression in the Mouse Olfactory System." *Journal of Comparative Neurology* 506, no. 2: 161–179. https://doi.org/10.1002/cne.21540.

Bokulich, N. A., B. D. Kaehler, J. R. Rideout, et al. 2018. "Optimizing Taxonomic Classification of Marker-Gene Amplicon Sequences With QIIME 2's q2-Feature-Classifier Plugin." *Microbiome* 6, no. 1: 90. https://doi.org/10.1186/s40168-018-0470-z.

Bolyen, E., J. R. Rideout, M. R. Dillon, et al. 2019. "Reproducible, Interactive, Scalable and Extensible Microbiome Data Science Using QIIME 2." *Nature Biotechnology* 37, no. 8: 852–857. https://doi.org/10.1038/s41587-019-0209-9.

Bray, E. R., M. Noga, K. Thakor, et al. 2017. "3D Visualization of Individual Regenerating Retinal Ganglion Cell Axons Reveals Surprisingly Complex Growth Paths." *eNeuro* 4, no. 4: ENEURO.0093-17.2017. https://doi.org/10.1523/ENEURO.0093-17.2017.

Bressel, O. C., M. Khan, and P. Mombaerts. 2016. "Linear Correlation Between the Number of Olfactory Sensory Neurons Expressing a Given Mouse Odorant Receptor Gene and the Total Volume of the Corresponding Glomeruli in the Olfactory Bulb." *Journal of Comparative Neurology* 524, no. 1: 199–209. https://doi.org/10.1002/cne.23835.

Bruce-Keller, A. J., J. M. Salbaum, M. Luo, et al. 2015. "Obese-Type Gut Microbiota Induce Neurobehavioral Changes in the Absence of Obesity." *Biological Psychiatry* 77, no. 7: 607–615. https://doi.org/10.1016/j.biopsych.2014.07.012.

Callahan, B. J., P. J. McMurdie, M. J. Rosen, A. W. Han, A. J. A. Johnson, and S. P. Holmes. 2016. "DADA2: High-Resolution Sample Inference From Illumina Amplicon Data." *Nature Methods* 13, no. 7: 581–583. https://doi.org/10.1038/nmeth.3869.

Caporaso, J. G., C. L. Lauber, W. A. Walters, et al. 2011. "Global Patterns of 16S rRNA Diversity at a Depth of Millions of Sequences Per Sample." *Proceedings of the National Academy of Sciences* 108, no. supplement_1: 4516–4522. https://doi.org/10.1073/pnas.1000080107.

Caporaso, J. G., C. L. Lauber, W. A. Walters, et al. 2012. "Ultra-High-Throughput Microbial Community Analysis on the Illumina HiSeq and MiSeq Platforms." *ISME Journal* 6, no. 8: 1621–1624. https://doi.org/10.1038/ismej.2012.8.

Cavallin, M. A., K. Powell, K. C. Biju, and D. A. Fadool. 2010. "State-Dependent Sculpting of Olfactory Sensory Neurons Is Attributed to Sensory Enrichment, Odor Deprivation, and Aging." *Neuroscience Letters* 483, no. 2: 90–95. https://doi.org/10.1016/j.neulet.2010.07.059.

Chandrasekaran, P., and R. Weiskirchen. 2024. "The Role of Obesity in Type 2 Diabetes Mellitus—An Overview." *International Journal of Molecular Sciences* 25, no. 3: 1882. https://doi.org/10.3390/ijms25031882.

Chao, A. 1987. "Estimating the Population Size for Capture-Recapture Data With Unequal Catchability." *Biometrics* 43, no. 4: 783–791. https://doi.org/10.2307/2531532.

Chelette, B. M., A. M. Loeven, D. N. Gatlin, et al. 2022. "Consumption of Dietary Fat Causes Loss of Olfactory Sensory Neurons and Associated Circuitry That Is Not Mitigated by Voluntary Exercise in Mice." *Journal of Physiology* 600, no. 6: 1473–1495. https://doi.org/10.1113/JP282112.

Costanzo, R. M., and M. Kobayashi. 2010. "Age-Related Changes in p2 Odorant Receptor Mapping in the Olfactory Bulb." *Chemical Senses* 35, no. 5: 417–426. https://doi.org/10.1093/chemse/bjq029.

Crain, E., D. M. Minaya, and C. B. de La Serre. 2025. "Microbiota-Induced Inflammation Mediates the Impacts of a Western Diet on Hippocampal-Dependent Memory." *Nutrition Research* 138: 89–106. https://doi.org/10.1016/j.nutres.2025.04.002.

D'Amato, A., L. Di Cesare Mannelli, E. Lucarini, et al. 2020. "Faecal Microbiota Transplant From Aged Donor Mice Affects Spatial Learning and Memory via Modulating Hippocampal Synaptic Plasticity- and Neurotransmission-Related Proteins in Young Recipients." *Microbiome* 8, no. 1: 140. https://doi.org/10.1186/s40168-020-00914-w.

de La Serre, C. B., C. L. Ellis, J. Lee, A. L. Hartman, J. C. Rutledge, and H. E. Raybould. 2010. "Propensity to High-Fat Diet-Induced Obesity in Rats Is Associated With Changes in the Gut Microbiota and Gut Inflammation." *American Journal of Physiology. Gastrointestinal and Liver Physiology* 299, no. 2: G440–G448. https://doi.org/10.1152/ajpgi.00098.2010.

Dougherty, B. 2002. Measure Stack (Version 1) [Computer Software].

Engin, A. B., and A. Engin. 2017. *Obesity and Lipotoxicity*. Vol. 960. Springer International Publishing. https://doi.org/10.1007/978-3-319-48382-5.

Fadool, D. A., K. Tucker, and P. Pedarzani. 2011. "Mitral Cells of the Olfactory Bulb Perform Metabolic Sensing and Are Disrupted

by Obesity at the Level of the Kv1.3 Ion Channel." *PLoS One* 6, no. 9: e24921. https://doi.org/10.1371/journal.pone.0024921.

Fardone, E., A. B. Celen, N. A. Schreiter, N. Thiebaud, M. L. Cooper, and D. A. Fadool. 2019. "Loss of Odor-Induced c-Fos Expression of Juxtaglomerular Activity Following Maintenance of Mice on Fatty Diets." *Journal of Bioenergetics and Biomembranes* 51, no. 1: 3–13. https://doi.org/10.1007/s10863-018-9769-5.

Fathi, M., A. Z. Javid, and A. Mansoori. 2023. "Effects of Weight Change on Taste Function; a Systematic Review." *Nutrition Journal* 22, no. 1: 22. https://doi.org/10.1186/s12937-023-00850-z.

Ferrario, C. R., H. Münzberg-Gruening, L. Rinaman, et al. 2024. "Obesity- and Diet-Induced Plasticity in Systems That Control Eating and Energy Balance." *Obesity* 32, no. 8: 1425–1440. https://doi.org/10.1002/oby.24060.

Harnischfeger, F., and R. Dando. 2021. "Obesity-Induced Taste Dysfunction, and Its Implications for Dietary Intake." *International Journal of Obesity* 45, no. 8: 1644–1655. https://doi.org/10.1038/s41366-021-00855-w.

Islam, M. A., A. B. Fagundo, J. Arcelus, et al. 2015. "Olfaction in Eating Disorders and Abnormal Eating Behavior: A Systematic Review." *Frontiers in Psychology* 6: 1431. https://doi.org/10.3389/fpsyg.2015.01431.

Johnson, M. C., K. C. Biju, J. Hoffman, and D. A. Fadool. 2013. "Odor Enrichment Sculpts the Abundance of Olfactory Bulb Mitral Cells." *Neuroscience Letters* 541: 173–178. https://doi.org/10.1016/j.neulet.2013.02.027.

Kadyan, S., G. Park, B. Wang, and R. Nagpal. 2023. "Dietary Fiber Modulates Gut Microbiome and Metabolome in a Host Sex-Specific Manner in a Murine Model of Aging." *Frontiers in Molecular Biosciences* 10: 1182643. https://doi.org/10.3389/fmolb.2023.1182643.

Kaufman, A., E. Choo, A. Koh, and R. Dando. 2018. "Inflammation Arising From Obesity Reduces Taste Bud Abundance and Inhibits Renewal." *PLoS Biology* 16, no. 3: e2001959. https://doi.org/10.1371/journal.pbio.2001959.

Kaufman, A., J. Kim, C. Noel, and R. Dando. 2020. "Taste Loss With Obesity in Mice and Men." *International Journal of Obesity* 44, no. 3: 739–743. https://doi.org/10.1038/s41366-019-0429-6.

Kelly, J. R., Y. Borre, C. O' Brien, et al. 2016. "Transferring the Blues: Depression-Associated Gut Microbiota Induces Neurobehavioural Changes in the Rat." *Journal of Psychiatric Research* 82: 109–118. https://doi.org/10.1016/j.jpsychires.2016.07.019.

Kim, J. S., R. A. Kirkland, S. H. Lee, et al. 2020. "Gut Microbiota Composition Modulates Inflammation and Structure of the Vagal Afferent Pathway." *Physiology & Behavior* 225: 113082. https://doi.org/10.1016/j.physbeh.2020.113082.

Kim, J. S., K. C. Williams, R. A. Kirkland, et al. 2023. "The Gut-Brain Axis Mediates Bacterial Driven Modulation of Reward Signaling." *Molecular Metabolism* 75: 101764. https://doi.org/10.1016/j.molmet.2023.101764.

Kim, Y. K., D. Jo, S. Choi, and J. Song. 2025. "High-Fat Diet Triggers Transcriptomic Changes in the Olfactory Bulb." *Heliyon* 11, no. 3: e42196. https://doi.org/10.1016/j.heliyon.2025.e42196.

Kimbrough, A., and O. George. 2020. *Brain Clearing (iDISCO) [Online Post]*. Protocols.Io. https://www.protocols.io/view/brain-clearing-idisco-rm7vz83b8vx1/v1.

Klug, M., E. Crain, A. Hayes, M. Shanmugam, C. de La Serre, and S. E. Kanoski. 2025. "Endotoxemia-Induced Inflammation in the Absence of Obesity Is Associated With Decreased Anxiety-Like and Impulsive Behavior With no Effect on Learning and Memory." *Comprehensive Physiology* 15, no. 5: e70044. https://doi.org/10.1002/cph4.70044.

Kobayashi, M., K. Nishida, K. Yamakata, and K. Takeuchi. 2025. "Aging Inhibits Olfactory Recovery From Traumatic Olfactory System Injury." *Neuroscience* 577: 64–70. https://doi.org/10.1016/j.neuroscience.2025.05.005.

Laursen, M. F. 2021. "Gut Microbiota Development: Influence of Diet From Infancy to Toddlerhood." *Annals of Nutrition and Metabolism* 77, no. Suppl. 3: 21–34. https://doi.org/10.1159/000517912.

Laursen, M. F., and H. M. Roager. 2023. "Human Milk Oligosaccharides Modify the Strength of Priority Effects in the *Bifidobacterium* Community Assembly During Infancy." *ISME Journal* 17, no. 12: 2452–2457. https://doi.org/10.1038/s41396-023-01525-7.

Laursen, M. F., M. Sakanaka, N. von Burg, et al. 2021. "*Bifidobacterium* Species Associated With Breastfeeding Produce Aromatic Lactic Acids in the Infant Gut." *Nature Microbiology* 6, no. 11: 1367–1382. https://doi.org/10.1038/s41564-021-00970-4.

Leary, S., W. Underwood, R. Anthony, et al. 2020. AVMA Guidelines for the Euthanasia of Animals: 2020 Edition. https://www.avma.org/sites/default/files/2020-0.2/Guidelines-on-Euthanasia-2020.pdf.

Ley, R. E., F. Bäckhed, P. Turnbaugh, C. A. Lozupone, R. D. Knight, and J. I. Gordon. 2005. "Obesity Alters Gut Microbial Ecology." *Proceedings of the National Academy of Sciences* 102, no. 31: 11070–11075. https://doi.org/10.1073/pnas.0504978102.

Li, N., Q. Wang, Y. Wang, et al. 2019. "Fecal Microbiota Transplantation From Chronic Unpredictable Mild Stress Mice Donors Affects Anxiety-Like and Depression-Like Behavior in Recipient Mice via the Gut Microbiota-Inflammation-Brain Axis." *Stress* 22, no. 5: 592–602. https://doi.org/10.1080/10253890.2019.1617267.

Liu, A., S. Savya, and N. N. Urban. 2016. "Early Odorant Exposure Increases the Number of Mitral and Tufted Cells Associated With a Single Glomerulus." *Journal of Neuroscience* 36, no. 46: 11646–11653. https://doi.org/10.1523/JNEUROSCI.0654-16.2016.

Liu, D., N. Archer, K. Duesing, G. Hannan, and R. Keast. 2016. "Mechanism of Fat Taste Perception: Association With Diet and Obesity." *Progress in Lipid Research* 63: 41–49. https://doi.org/10.1016/j.plipres.2016.03.002.

Loeven, A. M., A. N. Brown, F. U. Ebuara, K. M. Jones, and D. A. Fadool. 2025. "Both Obesogenic and Isocalorically-Controlled Diets Drive Changes in Microbiota Composition in a Sex-Dependent Manner in Mice." *Physiology & Behavior* 301: 115062. https://doi.org/10.1016/j.physbeh.2025.115062.

Lozovaya, N., S. Eftekhari, R. Cloarec, et al. 2018. "GABAergic Inhibition in Dual-Transmission Cholinergic and GABAergic Striatal Interneurons Is Abolished in Parkinson Disease." *Nature Communications* 9, no. 1: 1422. https://doi.org/10.1038/s41467-018-03802-y.

Lu, Y., G. Zhou, J. Ewald, Z. Pang, T. Shiri, and J. Xia. 2023. "MicrobiomeAnalyst 2.0: Comprehensive Statistical, Functional and Integrative Analysis of Microbiome Data." *Nucleic Acids Research* 51, no. W1: W310–W318. https://doi.org/10.1093/nar/gkad407.

Lusk, G., and E. F. Du Bois. 1924. "On the Constancy of the Basal Metabolism." *Journal of Physiology* 59, no. 2–3: 213–216. https://doi.org/10.1113/jphysiol.1924.sp002176.

Matiashova, L., A. L. Hoogkamer, and K. Timper. 2023. "The Role of the Olfactory System in Obesity and Metabolism in Humans: A Systematic Review and Meta-Analysis." *Metabolites* 14, no. 1: 16. https://doi.org/10.3390/metabo14010016.

McDonald, D., Y. Jiang, M. Balaban, et al. 2024. "Greengenes2 Unifies Microbial Data in a Single Reference Tree." *Nature Biotechnology* 42, no. 5: 715–718. https://doi.org/10.1038/s41587-023-01845-1.

Mobley, A. S., D. J. Rodriguez-Gil, F. Imamura, and C. A. Greer. 2014. "Aging in the Olfactory System." *Trends in Neurosciences* 37, no. 2: 77–84. https://doi.org/10.1016/j.tins.2013.11.004.

Moore, A. M., L. M. Coolen, and M. N. Lehman. 2019. "Kisspeptin/Neurokinin B/Dynorphin (KNDy) Cells as Integrators of Diverse Internal and External Cues: Evidence From Viral-Based Monosynaptic

Tract-Tracing in Mice." *Scientific Reports* 9, no. 1: 14768. https://doi.org/10.1038/s41598-019-51201-0.

Nagpal, R., S. P. Mishra, and H. Yadav. 2020. "Unique Gut Microbiome Signatures Depict Diet-Versus Genetically Induced Obesity in Mice." *International Journal of Molecular Sciences* 21, no. 10: 3434. https://doi.org/10.3390/ijms21103434.

Peinado, B. R. R., D. R. Frazão, L. O. Bittencourt, et al. 2023. "Is Obesity Associated With Taste Alterations? A Systematic Review." *Frontiers in Endocrinology* 14: 1167119. https://doi.org/10.3389/fendo.2023.1167119.

Peng, M., D. Coutts, T. Wang, and Y. O. Cakmak. 2019. "Systematic Review of Olfactory Shifts Related to Obesity." *Obesity Reviews* 20, no. 2: 325–338. https://doi.org/10.1111/obr.12800.

Potter, S. M., C. Zheng, D. S. Koos, P. Feinstein, S. E. Fraser, and P. Mombaerts. 2001. "Structure and Emergence of Specific Olfactory Glomeruli in the Mouse." *Journal of Neuroscience* 21, no. 24: 9713–9723. https://doi.org/10.1523/JNEUROSCI.21-24-09713.2001.

Proserpio, C., M. Laureati, S. Bertoli, A. Battezzati, and E. Pagliarini. 2015. "Determinants of Obesity in Italian Adults: The Role of Taste Sensitivity, Food Liking, and Food Neophobia." *Chemical Senses* 41, no. 2: 169–176. https://doi.org/10.1093/chemse/bjv072.

Renier, N., Z. Wu, D. J. Simon, J. Yang, P. Ariel, and M. Tessier-Lavigne. 2014. "iDISCO: A Simple, Rapid Method to Immunolabel Large Tissue Samples for Volume Imaging." *Cell* 159, no. 4: 896–910. https://doi.org/10.1016/j.cell.2014.10.010.

Ridaura, V. K., J. J. Faith, F. E. Rey, et al. 2013. "Gut Microbiota From Twins Discordant for Obesity Modulate Metabolism in Mice." *Science (New York, N.Y.)* 341, no. 6150: 1241214. https://doi.org/10.1126/science.1241214.

Salinero, A. E., B. M. Anderson, and K. L. Zuloaga. 2018. "Sex Differences in the Metabolic Effects of Diet-Induced Obesity Vary by Age of Onset." *International Journal of Obesity* 42, no. 5: 1088–1091. https://doi.org/10.1038/s41366-018-0023-3.

Sato, T., R. Homma, and S. Nagayama. 2020. "Direct Comparison of Odor Responses of Homologous Glomeruli in the Medial and Lateral Maps of the Mouse Olfactory Bulb." *eNeuro* 7, no. 2: ENEURO.0449-19.2020. https://doi.org/10.1523/ENEURO.0449-19.2020.

Schindelin, J., I. Arganda-Carreras, E. Frise, et al. 2012. "Fiji: An Open-Source Platform for Biological-Image Analysis." *Nature Methods* 9, no. 7: 676–682. https://doi.org/10.1038/nmeth.2019.

Şeref, B., and H. Yıldıran. 2024. "A New Perspective on Obesity: Perception of Fat Taste and Its Relationship With Obesity." *Nutrition Reviews* 83, no. 2: e486–e492. https://doi.org/10.1093/nutrit/nuae028.

Shannon, C. E. 1948. "A Mathematical Theory of Communication." *Bell System Technical Journal* 27, no. 3: 379–423. https://doi.org/10.1002/j.1538-7305.1948.tb01338.x.

Thaiss, C. A., M. Levy, T. Korem, et al. 2016. "Microbiota Diurnal Rhythmicity Programs Host Transcriptome Oscillations." *Cell* 167, no. 6: 1495–1510.e12. https://doi.org/10.1016/j.cell.2016.11.003.

Thaiss, C. A., D. Zeevi, M. Levy, et al. 2014. "Transkingdom Control of Microbiota Diurnal Oscillations Promotes Metabolic Homeostasis." *Cell* 159, no. 3: 514–529. https://doi.org/10.1016/j.cell.2014.09.048.

Thiebaud, N., M. C. Johnson, J. L. Butler, et al. 2014. "Hyperlipidemic Diet Causes Loss of Olfactory Sensory Neurons, Reduces Olfactory Discrimination, and Disrupts Odor-Reversal Learning." *Journal of Neuroscience: The Official Journal of the Society for Neuroscience* 34, no. 20: 6970–6984. https://doi.org/10.1523/JNEUROSCI.3366-13.2014.

Todrank, J., G. Heth, and D. Restrepo. 2011. "Effects of *in Utero* Odorant Exposure on Neuroanatomical Development of the Olfactory Bulb and Odour Preferences." *Proceedings of the Royal Society B: Biological Sciences* 278, no. 1714: 1949–1955. https://doi.org/10.1098/rspb.2010.2314.

Tofani, G. S. S., S.-J. Leigh, C. E. Gheorghe, et al. 2025. "Gut Microbiota Regulates Stress Responsivity via the Circadian System." *Cell Metabolism* 37, no. 1: 138–153.e5. https://doi.org/10.1016/j.cmet.2024.10.003.

Trius-Soler, M., D. A. Santillán-Alarcón, M. Martínez-Huélamo, R. M. Lamuela-Raventós, and J. J. Moreno. 2020. "Effect of Physiological Factors, Pathologies, and Acquired Habits on the Sweet Taste Threshold: A Systematic Review and Meta-Analysis." *Comprehensive Reviews in Food Science and Food Safety* 19, no. 6: 3755–3773. https://doi.org/10.1111/1541-4337.12643.

Tucker, K., M. A. Cavallin, P. Jean-Baptiste, et al. 2010. "The Olfactory Bulb: A Metabolic Sensor of Brain Insulin and Glucose Concentrations via a Voltage-Gated Potassium Channel." *Results and Problems in Cell Differentiation* 52: 147–157. https://doi.org/10.1007/978-3-642-14426-4_12.

Tucker, K., and D. A. Fadool. 2002. "Neurotrophin Modulation of Voltage-Gated Potassium Channels in Rat Through TrkB Receptors Is Time and Sensory Experience Dependent." *Journal of Physiology* 542, no. Pt 2: 413–429. https://doi.org/10.1113/jphysiol.2002.017376.

Tucker, K., J. M. Overton, and D. A. Fadool. 2012. "Diet-Induced Obesity Resistance of Kv1.3−/− Mice Is Olfactory Bulb Dependent." *Journal of Neuroendocrinology* 24, no. 8: 1087–1095. https://doi.org/10.1111/j.1365-2826.2012.02314.x.

Turnbaugh, P. J., F. Bäckhed, L. Fulton, and J. I. Gordon. 2008. "Diet-Induced Obesity Is Linked to Marked but Reversible Alterations in the Mouse Distal Gut Microbiome." *Cell Host & Microbe* 3, no. 4: 213–223. https://doi.org/10.1016/j.chom.2008.02.015.

Turnbaugh, P. J., R. E. Ley, M. A. Mahowald, V. Magrini, E. R. Mardis, and J. I. Gordon. 2006. "An Obesity-Associated Gut Microbiome With Increased Capacity for Energy Harvest." *Nature* 444, no. 7122: 1027–1031. https://doi.org/10.1038/nature05414.

Valle-Leija, P., E. Blanco-Hernández, R. Drucker-Colín, G. Gutiérrez-Ospina, and R. Vidaltamayo. 2012. "Supernumerary Formation of Olfactory Glomeruli Induced by Chronic Odorant Exposure: A Constructivist Expression of Neural Plasticity." *PLoS One* 7, no. 4: e35358. https://doi.org/10.1371/journal.pone.0035358.

Zheng, C., P. Feinstein, T. Bozza, I. Rodriguez, and P. Mombaerts. 2000. "Peripheral Olfactory Projections Are Differentially Affected in Mice Deficient in a Cyclic Nucleotide-Gated Channel Subunit." *Neuron* 26, no. 1: 81–91. https://doi.org/10.1016/s0896-6273(00)81140-x.

Zhou, Z., and L. Belluscio. 2012. "Coding Odorant Concentration Through Activation Timing Between the Medial and Lateral Olfactory Bulb." *Cell Reports* 2, no. 5: 1143–1150. https://doi.org/10.1016/j.celrep.2012.09.035.

Zhu, Y., B. Chen, X. Zhang, et al. 2024. "Exploration of the *Muribaculaceae* Family in the Gut Microbiota: Diversity, Metabolism, and Function." *Nutrients* 16, no. 16: 2660. https://doi.org/10.3390/nu16162660.

Supporting Information

Additional supporting information can be found online in the Supporting Information section. **Data S1:** jnc70396-sup-0001-FigureS1-S3.pdf.